SRNL-STI-2012-00387
Revision 0

Keywords: *HB-Line, AFS-2, Purification, Anion Exchange, Specification, MOX*

Retention: *Permanent*

Plutonium Loading Capacity of Reillex™ HPQ Anion Exchange Column - AFS-2 Plutonium Flowsheet for MOX

E. A. Kyser
W. D. King
P. E. O'Rourke

July 2012

Savannah River National Laboratory
Savannah River Nuclear Solutions
Aiken, SC 29808

Prepared for the U.S. Department of Energy under contract number DE-AC09-08SR22470.

SRNL
SAVANNAH RIVER NATIONAL LABORATORY

DISCLAIMER

Printed in the United States of America

Prepared for
U.S. Department of Energy

AUTHORS:

original approved by E. A. Kyser *7/26/2012*

E. A. Kyser Date
Separations and Actinide Science Programs

original approved by W. D. King *7/25/2012*

W. D. King Date
Advanced Characterization and Process

original approved by Patrick O'Rourke *7/26/2012*

P. E. O'Rourke Date
Analytical Development

TECHNICAL REVIEW:

original approved Tracy S. Rudisill *7/27/2012*

T. S. Rudisill Date
Separations and Actinide Science Programs

APPROVAL:

original approved by Samuel D. Fink *8/1/2012*

S. D. Fink, Manager Date
Separations and Actinide Science Programs

original approved by Bill Giddings for *8/2/2012*

S. L. Marra, Manager Date
Environmental & Chemical Process Technology Research Programs

original approved by K.P. Burrows *8/2/2012*

K. P. Burrows, Manager Date
HB-Line Engineering

Table of Contents

List of Figures:

List of Tables:

Plutonium Loading Capacity of Reillex™ HPQ Anion Exchange Column - AFS-2 Plutonium Flowsheet for MOX

SUMMARY

Radioactive plutonium (Pu) anion exchange column experiments using scaled HB-Line designs were performed to investigate the dependence of column loading performance on the feed composition in the H-Canyon dissolution process for plutonium oxide (PuO_2) product shipped to the Mixed Oxide (MOX) Fuel Fabrication Facility (MFFF).

These loading experiments show that a representative feed solution containing ~5 g Pu/L can be loaded onto Reillex™ HPQ resin from solutions containing 8 M total nitrate and 0.1 M KF provided that the F is complexed with Al to an [Al]/[F] molar ratio range of 1.5-2.0. Lower concentrations of total nitrate and [Al]/[F] molar ratios may still have acceptable performance but were not tested in this study. Loading and washing Pu losses should be relatively low (<1%) for resin loading of up to 60 g Pu/L. Loading above 60 g Pu/L resin is possible, but Pu wash losses will increase such that 10-20% of the additional Pu fed may not be retained by the resin as the resin loading approaches 80 g Pu/L resin.

BACKGROUND

HB-Line Engineering requested that SRNL develop an anion exchange flowsheet[1] for the purification of Pu dissolved in H-Canyon to meet the Interface Control Document (ICD) limits[2] for the Mixed Oxide MOX Fuel Fabrication Facility (MFFF) (see Table 1). Three levels of limits are given: 1) Column B, 2) Column A and 3) Exceptional. The proposed feedstock to this process is part of an inventory characterized as Alternate Feedstocks 2 (AFS-2) and consists of Pu metal from multiple sources.

The major impurities expected in the feed to HB-Line are primarily those added during the dissolution process in H-Canyon[3] (i.e., Gd or B, potassium (K), fluoride (F), iron (Fe) and aluminum (Al)). Gallium (Ga) is also a major impurity as it comprises a significant component in the AFS-2 feedstock. After the Pu metal is dissolved in H-Canyon, HB-Line will perform anion exchange, oxalate precipitation, filtration and calcination to produce a plutonium dioxide (PuO_2) product. The primary purification will be performed by anion exchange but additional purification will be obtained by precipitation, filtration and calcination for some impurities.

In a previous study, Kyser[4] determined that none of the major impurities had a large affinity for the resin but that the rare earths had enough affinity that purification to the proposed ICD limits would have been difficult. Boron was therefore recommended for the process when a neutron poison was required. In the current study, Pu loading experiments were performed to investigate the effect of Al, F, B and total NO_3^- on the capacity of the column. Because Pu forms strong complexes with F and because of the corrosion potential of F on process equipment, historical anion exchange operation has relied on using a large excess of Al to complex the F and avoid issues with Pu losses and corrosion. SRS has commonly used a molar [Al]/[F] ratio of 3 or 4 to 1. LANL has documented an investigation[5] where they studied [Al]/[Pu] ratios of 0.1 to 10 and [F]/[Al] ratios of 0 to 6 and observed significant impacts of F on the Pu Kd for Lewatit® MP-500-FK anion resin.

This report documents ion exchange column experiments aimed at determining the loading behavior of Pu onto the anion resin column and the amount of Pu losses that should be expected for loading up to ~70 g Pu/L resin from representative feed solutions containing F, Al, B and Fe.

Impurity Removal by Anion Exchange: James[6] and Marsh[7] each provide a periodic table viewpoint on the affinity of various elements for a nitrate anion exchange system. Each author interpreted the data available to them in a different fashion. A modified version of the periodic table from Marsh is included as Figure 1 with color coding to show the expected and potential process impurities that have been identified. Note that none of the major impurities identified in the AFS-2 feed show significant affinity for the resin.

---

[1] J. W. Christopher, "Flowsheet Development for HB-Line Phase II Oxide Production," NMMD-HTS-2011-3177, Revision 0 (Nov 10, 2011).
[2] Mixed Oxide Fuel Fabrication Facility (MFFF) – H-Area/K-Area Plutonium Dioxide Powder Interface Control Document, ICD-11-032-01, G-ESR-H-00189, Rev. 0, 05/31/2012.
[3] T. S. Rudisill, R. A. Pierce, "Dissolution of Plutonium Metal in 8-10 M Nitric Acid", SRNL-STI-2012-00043, Rev. 1, Savannah River National Laboratory, Aiken SC, July, 2012.
[4] E. A. Kyser, W. D. King, "HB-Line Anion Exchange Purification of AFS-2 Plutonium for MOX", SRNL-STI-2012-00233, Rev. 0, Savannah River National Laboratory, Aiken SC, April 2012.
[5] S. F. Marsh, "The Effect of Fluoride and Aluminum on the Anion Exchange of Plutonium from Nitric Acid", LA-10999, Los Alamos National Laboratory, Los Alamos, NM (July 1987).
[6] D. B. James, "Anion Exchange Processing of Plutonium", LA-3499, Los Alamos Scientific Laboratory, Los Alamos, NM, January 4, 1966.
[7] S. F. Marsh, "Evaluation of a New Macroporous Polyvinylpyridine Resin for Processing Plutonium Using Nitrate Anion Exchange", LA-11490, Los Alamos National Laboratory, Los Alamos, NM (April 1989).

Process Scaling: Plant scale anion exchange equipment is typically 100 to 1000 times larger than laboratory equipment. Normally the process is scaled based on the linear velocity (Q/A, mL/min/cm^2 = cm/min) through the resin bed (which is related to residence time in the bed) and the loading profile of the resin. If a laboratory column contains resin at the same depth as the plant equipment, then scaling is primarily reduced to one of flow area and Pu flux through the bed (ensuring linear velocity will be the same). Higher Pu concentrations in the feed solution will produce a higher Pu resin loading. Lower flowrates would also tend to increase the effective loading by increasing the time for mass transfer. The HB-Line Pu anion columns nominally hold a 27-inch tall cylinder of resin with a 7.62-in ID (294.1-cm^2 cross sectional area) which contains ~20.1 L of resin[8,9]. These experiments used a two segment 27-in (68.6 cm) tall laboratory column (12.6-mm ID or 1.247 cm^2) previously used in the Pu DF experiments.[4] This column consisted of two segments which contained a total of 85.5 cm^3 of resin and was operated at flowrates as shown in Table 2. The targeted flowrate of 4.5 mL/min at 4.5 g Pu/L for a 1.247-cm^2 laboratory column was based on a cross-sectional area for the HB-Line column of 294.1 cm^2 (7.62-in ID) and process loading rates of 1.1 L/min at 4.5 g Pu/L[8,10,11,12]. This loading rate corresponds to ~17 mg Pu/min/cm^2. To be bounding, the Pu feed concentration for these tests was a minimum of 4.5 g Pu/L. Higher Pu feed concentrations could result in a marginally higher amount of Pu losses. Table 2[13] shows a comparison between the proposed HB-Line operating conditions, and current and previous[4] SRNL test conditions.

Effect of Resin Aging: The effect of aging of the resin was not tested in this study. In past work[7,8] it was reported that Reillex™ HPQ Pu loading capacity would tend to initially increase with chemical or radiolytic exposure due to opening of the resin structure. The actual loading sites were not seriously impacted until significant damage had been done to the resin due to stabilization by the pyridine ring structure. Eventually, the loading capacity would drop with significant exposure. Gamma radiation exposure of 100 MRad did not appear to have a negative effect on Pu loading capacity.[8] Similarly, short term heating to 85 °C for 30 min in 8 M HNO_3 generated NO_x fumes but also did not appear to have a negative effect on Pu loading capacity.[8] Based on these previous observations, it is considered likely that resin capacity will not be seriously reduced until after a relatively significant amount of processing has been performed.

[8] E. A. Kyser, "Plutonium Loading onto Reillex™ HPQ Anion Exchange Resin", WSRC-TR-2000-00372, Westinghouse Savannah River Company, Aiken, SC (Sept 26, 2000).
[9] Drawing W720067 R45, "Savannah River Plant, Bldg 221H, 8 Inch Dia. Co lumn Assembly Process, H363-110-1,2,3 & 4", (January 29, 1985).
[10] Drawing W720279 R0, "Savannah River Plant, Bldg 221H, Nept. 237, Plut. 239 Flow Diagram Process", (July 31,1981).
[11] Drawing W743159 R25, "Savannah River Plant, Bldg 221H, Enhancement of Pu 239 Capability, Flow Diagram Sh. No. 2 Process", (March 1, 1985).
[12] R. H. Smith, "HB-Line Pu-239 Production Flow Sheet Strategy", SRNS-E-1100-2011-00025, Rev. 1, (January 23, 2012).
[13] E. A. Kyser,"Task Technical and Quality Assurance Plan for Plutonium Anion Exchange Flowsheet for HB-Line", SRNL-RP-2011-01598, Savannah River National Laboratory, Aiken SC, December 2011.

EXPERIMENTAL

Column Experiments: Three Pu column loading tests were performed with a two-piece column installed in a glovebox. The two-piece column was necessary to achieve the required resin-bed height due to the limited height of the glovebox. Tests were performed to evaluate the effects of nitric acid concentration and [Al]/[F] ratio on column loading performance and Pu losses.

Resin Pretreatment: The Reillex™ HPQ resin that was tested came from the 1998 manufacturer's lot (#80302MA) that was purchased by SRNL for Pu flowsheet work[14] and later used for Np flowsheet work. All resin was initially converted from the chloride form (as-shipped) to the nitrate form by washing with 1 M $NaNO_3$ (Washing with ~10 BV in a column was the preferred method for conversion, but other methods are acceptable). The assembled column was thoroughly washed with 8 M HNO_3 prior to the start of the experiments.

Column Preparation: A sufficient quantity of resin was converted into the nitrate form prior to loading the column. The resin was loaded into the column as a resin-water slurry to avoid air entrainment in the bed. The resin bed was settled by passing water (or dilute HNO_3) down-flow through the resin bed. No obvious gaps or void spaces were visible. The final resin bed volume was adjusted by adding a small amount of resin or removing excess resin with a slurry pipette to obtain the desired resin bed height. A 100 mesh 304L screen (see Figures 2a, and 2b) was installed above and below the packed bed to retain the resin and allow for up-flow operation. This screen fit tightly within the column body and did not allow the resin bed to expand significantly. The screen also prevented upward flow from fluidizing the resin bed. Volume changes of the resin beads and the packed bed are insignificant during processing once the resin is in the nitrate form, but retained gas bubbles would cause the resin bed to expand without the screen installed. Gas bubbles trapped within the moist bed are often very difficult to remove and will cause channeling of the flow through the bed. A tightly held resin bed does not allow channeling to occur. The columns and resin bed used in this testing were also used for two previous Pu column tests focused on Pu product impurity levels described in a separate report[4].

Lab Equipment: The Pu experiments involved a two-piece column design (due to limited headroom in the glovebox) that used ¼ and 1/8-in polypropylene tubing to connect to the 12.6-mm ID glass body (Figure 2b). Teflon™ bushings (#7) were used to attach the columns to the polypropylene tubing. The headpiece was attached to the right column with a Rodaviss™ joint to allow the column to retain a larger pressure head than allowed by a standard ground glass joint. As a safety precaution, the headpiece also had an Ace Glass, Inc. pressure-relief valve. An additional arm allowed the column to be vented. The bottom of the left column (which serves as the effective bottom of the entire column) had a 3-way Swagelok™ valve installed to change the flow direction from up-flow to down-flow. The bottom of the right column was connected to the top of the left column with 1/8-in tubing. The top and bottom of both columns used 12-mm diameter-100 mesh screen (similar to that shown in Figure 2a) to retain the resin. A sketch of the experimental setup for the up-flow load/wash steps is shown as Figure 3 for a representative 1-piece column. A separate sketch of the down-flow elution experimental setup is shown as Figure 4. Figures 3 and 4 also show the installation of flowcells and fiber optics that were used for continuous spectroscopic analysis during the loading and wash portions of these experiments, but not during elution. The feed line was connected to the bottom of the left column during the condition, load and wash steps and then changed to the top of the right column for the elution step (along with switching the 3-way valve to the elution position). A standard FMI (Fluid Metering, Inc.) piston pump was used to pump feed, wash, or elution acid through the column. In

[14] W. J. Crooks, E. A. Kyser, S. R. Walters, "Qualification of Reillex™ HPQ Anion Exchange Resin for Use in SRS Processes", WSRC-TR-99-00317, Westinghouse Savannah River Company, Aiken, SC (March 10, 2000).

some instances, interruptions in the flow made the flowrate determination inaccurate. Since the flowrate was not easy to monitor as the experiment was performed, some flowrates (particularly during elution) were lower than intended, but the wash and elution volumes collected were well known.

A ½-in Swagelok™ cross and two ½-in optic lenses were used to fabricate a flowcell with a 23.52-mm path length that was used to observe dilute Pu solution exiting from the column during the load/wash steps. A 1 mm flowcell for use during the elution step was fabricated by welding 3/16-in tubing into a ½-in Swagelok™ union and milling out the union to allow two ½-in optic lenses to slide to the center. The 1-mm cell was not used during this study. The 23.52-mm cell with lenses is shown unassembled and assembled in Figure 5. Two pairs of fiber optic lines previously installed through the ceiling of the glovebox allowed a light signal to be brought into the glovebox, passed through the flowcell and carried out to an Avantes spectrometer controlled by a computer. A detailed equipment list for the complete spectrophotometer system is given in Table 3. Reference and measurement spectra were taken on the same pair of UV grade fibers. Light references were taken prior to the beginning of the experiment and stored. Raffinate spectra were taken over time during both the loading and wash steps of each experiment. Observations recorded during the experiment allowed the calculation of the volume associated with each spectrum. Fibers could be switched at the lamp and spectrometer after the wash step to allow measurement of the elution profile with the 1-mm flowcell in a similar manner. In this study, the 1-mm flowcell was not installed and all elution cuts were made by visual observation only.

Sample spectra were also measured in 1 cm disposable cuvettes in a plexiglass holder in the glovebox which also used fiber optic lines to connect to the light source and spectrometer.

Feed Matrix: A feed matrix was prepared which contained the primary AFS-2 metal feedstock components (e.g. B and Al) that are expected to influence the speciation of Pu and F. Because of the history of the Pu used in these experiments, ferrous sulfamate (FS) was used as valence adjustment in this laboratory work whereas it is not planned for use in the production process. Ferric nitrate was used as a source of additional Fe to match the planned flowsheet concentrations. Other impurities (such as Ga) were not included as their influence on the loading of Pu is expected to be minor. It is assumed that they would weakly compete to complex F^- and their absence is conservative in this study since a higher concentration of F may be available to complex Pu (which would increase losses).

Analytical Methods: Gamma counting (Gamma Scan) and alpha plate counting (Alpha PHA) were used to measure Pu and Am and perform a material balance. Impurities such as Al, F, Fe and B were primarily measured by the weight of the reagents added, although analytical confirmation was attempted. Inductively-coupled plasma emission spectroscopy (ICPES) was used to measure B, Al, K, Fe and S, and IC Anions was used to measure F^- and NO_3^-. Feed samples were analyzed in triplicate by acid titration with hydroxide. Since species such as Pu, Al and Fe also titrated, both the Analytical Development (AD) Free and Total acid methods were used to characterize feed samples for each experiment. Samples for submission to ICPES were submitted in plastic vials due to past Na, B, Si and Al contamination issues that appeared to be associated with the glass sample vials which are commonly used.

Reagents: Reagent grade chemicals were generally used with the exception of ferrous sulfamate (FS); H-Area plant production FS was used. The purity of the reagents for the preparation of the feed solution was not a significant concern. Deionized water and reagent grade HNO_3 were used for all preparations.

MODELING

Multivariate Modeling Background: This work relies heavily on the use of UV-visible spectroscopy to perform at-line solution analyses of the column raffinate. The fundamental relationship between the absorption of light by transparent materials and their chemical composition is expressed in the Beer-Lambert law:

$$(1)\ I(\lambda)=I_o(\lambda)*exp(-\varepsilon(\lambda)*c*x)$$

where $I(\lambda)$ is the final intensity of the light beam as a function of wavelength, $I_o(\lambda)$ is the initial intensity of the light beam, $\varepsilon(\lambda)$ is the molar absorptivity of a chemical species (all of which in principle are known constants), c is the concentration of the chemical species, and x is the path-length of the optical cell (which is fixed).

For systems with multiple chemical species:

$$(2)\ I(\lambda) = I_o(\lambda) * \exp\left(-x * \sum_i^N (\varepsilon_i(\lambda) * c_i)\right).$$

The quantity Absorbance is defined:

$$(3)\ A = -Log\left(\frac{I}{I_o}\right).$$

So:

$$(4)\ A(\lambda) = 2.303 * x * \sum_i^N (\varepsilon_i(\lambda) * c_i).$$

This is a set of coupled linear equations which can be represented as a matrix equation:

$$(5)\ [A] = k * [E] * [C].$$

This equation can be inverted using any one of several methods from linear algebra as suggested by Martens[15],Wold[16],or Thomas[17] to calculate chemical concentration from a measured absorbance spectrum.

We used the method of Principle Component Regression (PCR) to calibrate the spectrophotometer for Pu concentration. To perform the calibration, we measured the spectra from a set of Pu standard solutions with varying Pu, F, NO_3^-, H^+, and Fe concentrations. The spectra, however, exhibited significant baseline shifts. The shifts were eliminated by convolving the raw absorbance spectra with a Gaussian weighted second-derivative kernel[18]:

$$(6)\ SD(\lambda) = \sum_{i=-n}^{n} (SDG(i,\sigma) * A(\lambda + i))$$

where $SD(\lambda)$ is the processed second derivative spectra, and $SDG(i,\sigma)$is the convolution kernel. The formula used to generate the kernel function is:

$$(7)\ SDG(i,\sigma) = \frac{1}{\sqrt{2\pi}\,\sigma} * \frac{i^2 - \sigma^2}{\sigma^4} * e^{-\frac{1}{2}*\left(\frac{i}{\sigma}\right)^2}.$$

We set σ = 5, which corresponds to the 2-nm band-pass of the spectrometer, and used a value of n=50 for the kernel extent. Data processing and graphics functions are implemented through macros and worksheet functions in Microsoft Excel workbooks 'Aventes_Model.xls' and 'Process_Spec-

[15] *Multivariate Calibration*, H. Martens and T. Neas, John Wiley & Sons, 1991.
[16] *The Multvariate Calibration Problem in Chemistry Solved by the PLS Method*, S. Wold, H. Martens and H. Wold, Lecture Notes in Mathematics, 1983, Vol. 973, pp 286-293.
[17] E. V. Thomas, D. M. Haaland, "Comparison of Multivariate Calibration Methods for Quantitative Spectral Analysis, Anal. Chem., 1990, Vol. 62, pp 1091-1099.
[18] M. F. Merrick and H. L. Pardue, "Evaluation of Absorption and First- and Second-Derivative Spectra for Simultaneous Quantification of Bilirubin and Hemoglobin", Clin. Chem. 1986, Vol. 32/4, pp 598-602.

trum.xlsm'.[19] A flow diagram of this process is shown in Figure 6. Raw spectral data from the plutonium standards were collected into the workbook and mathematically processed before being translated into a format useable by the modeling program. After modeling, the resulting parameter files then had to be translated back into a Microsoft Excel compatible format so model predictions could be made from the set of spectra.

Development of Prediction Models from Spectra: In a previous loading study, Kyser[8] used SRNL developed software programs to acquire and mathematically process spectra using the SRNL-AD developed SRLMVA (Savannah River Laboratory Multivariate Analysis) program. The current equipment saves the spectral data in a Microsoft Excel spreadsheet format. Macro routines were developed to perform the bulk of the mathematical calculations within Microsoft Excel as was previously described. Second derivative preprocessing was performed on each spectrum and the modeled wavelength range was generally limited to 450 to 850 nm to avoid noise and interferences. At the current time, the capability to fit the model parameters only exists in the DOS MVA.exe program (MVA-Multivariate Analysis), so the spectral standard data had to be transferred to MVA format to perform the modeling and the resulting model had to be transferred back into Microsoft Excel to allow predictions using the spectra from the experiments. Because of the limitation of operating the MVA program in a DOS window; it has severe memory limitations by today's standards. By limiting the number of calibration spectra and the wavelength range of interest, usable models were developed. These models were used within Microsoft Excel to predict Pu concentrations for spectra saved from each experiment.

Each experiment involved a variation in [F], [Al]/[F] molar ratio or the total nitrate concentration. The effect of the variation in the solution matrix on the Pu spectra was incorporated in the models by measuring the spectra of dilutions of the feed solution with a "Spectral Dilution" solution which attempted to match the composition of feed solution (but without Pu present). Spectra of the undiluted feed solution were measured, along with 5X, 21X, 51X and 126X dilutions of the feed solution with the spectral dilution. Gamma counting of the initial solution was used to determine the Pu concentration and all dilutions were performed using a combination of volumetric and gravimetric measurements. When the spectral dilution solution contained FS, it was recognized that the Fe^{2+} required oxidation to Fe^{3+} prior to preparation of the dilutions to avoid the reduction of the Pu^{4+} to Pu^{3+}. A "heat-kill" of 30 minutes at 50 °C was used for this purpose. Since these experiments involved the observation of Pu losses during the wash step, a separate Pu^{4+} standard solution along with similar dilutions in 8 M HNO_3 were prepared and the spectra measured. Spectra for the initial experiment were prepared from a surrogate "Cr315 Pu Standard" solution that was prepared after the Cr315 experiment was completed because sufficient Cr315 feed solution was not available to prepare the dilutions. Figure 7 shows the spectra of the feed solutions and standards used to prepare the dilutions (Table 4) that form the bases for the models. Multiple spectra of the four dilutions of each solution were measured along with the feed solution and the spectral dilution solution.

Principal component regression (PCR) models for each set of spectral standards were prepared along with combinations of spectra in an attempt to find the most appropriate method of modeling the data and predicting the Pu concentration of the raffinate from each experiment. For each experiment there was an initial phase where only Fe^{3+} and Am^{3+} were visible in the spectra. The point where Pu^{4+} in the raffinate was initially detected was identified by visual inspection and all Pu concentrations before that point were assigned a value of zero. During this initial break-through phase the most relevant spectra for prediction tended to be those prepared from the feed solution. After the wash solution removed the bulk of the Am, F and Fe from the column, then the spectra from the Pu^{4+} standard became

[19] P. E. O'Rourke, Numerical Data Analysis for AD, SRNL-NB-2012-00082, Savannah River National Laboratory, Aiken, SC July 2012.

the most relevant spectra for prediction. In all cases the highest concentration solution and the initial, 5X dilution appeared to dominate the models (and were predicted to within 1%) but dilute standards were typically predicted by the models to within 10% down to 0.02 g Pu/L.

RESULTS

Effect of [Al]/[F] Ratio on Pu-F Complexation: To estimate the amount of Al needed to sufficiently complex the F to avoid an effect on the Pu resin performance, a series of test solutions containing F, B, Gd, Al and Pu in 7-8 M HNO_3 were prepared. Careful choice of reagent concentrations allowed accurate preparation of small volumes (~4 mL) of various mixtures of impurities (using standard pipets) all at the same Pu and HNO_3 concentration but with varying concentrations of impurities. Table 5 shows the concentrations of the various solutions used in the preparation of a series of mixtures listed in Table 6. These solutions were prepared and then the UV-visible spectrum was measured using disposable 1 cm cuvettes. Comparison of the absorbance spectra and mathematical derivatives of those spectra allowed the effect of F on the Pu spectra to be observed in the various solution mixtures.

Pu^{4+} in 8M HNO_3 was used as a comparison knowing the high affinity that $Pu(NO_3)_6^{2-}$ has for strong base anion resin such as Reillex™ HPQ. Differences between the spectra of pure Pu^{4+} nitrate solution and the F-containing matrices are presumed to be an indication of Pu speciation differences that pose a negative effect on anion exchange loading capacity. Figure 8 shows the effect of increasing F concentration on the Pu spectra relative to pure plutonium nitrate solution (bold green in Figure 8). Note that while there are many observed differences in the spectra of the Pu-F solutions, the increase in F concentration from 0.1 to 0.8 M KF ([Pu]/[F] molar ratios of 2.7 to 21) did not alter the spectra significantly. Figure 9 shows the effect of 0.2 g/L (1.33 mM) Gd and 1 g/L B (94mM) as boric acid on the Pu-F spectra. At these concentrations neither Gd nor B had a significant effect on the spectra of Pu-F. Also shown in Figure 9 is the effect of 0.045 and 0.1 M Al ([Al]/[F] ≈ 1 and 2) on the Pu-F spectra with 0.2 g Gd/L present. Clearly the 2:1 [Al]/[F]-spectrum has much less of the character of the other Pu-F spectra and this spectrum is approaching that of pure Pu^{4+} in 8M HNO_3. Based on this result, a tentative [Al]/[F] ratio of 2 was chosen as the initial target value for this study and depending on the results from the initial testing at this condition, other less favorable conditions were then considered for testing.

Feed Preparation: Feed solutions were prepared by dissolving reagents into water as shown in Table 7. Nitrate salts were used as the source of most impurities. Analyzed results for each feed solution are shown in Table 8. The H-Canyon minimum B concentration[20] of 1.2 g B/L was the target for all feed solutions. Additional boric acid would provide additional competition for complexation of F. The effect of increased B concentration on the Pu resin loading would be expected to be positive, although that effect may not be significant. It was planned to test the effect of lower [Al]/[F] molar ratio and lower total [NO_3^-] to investigate the sensitivity of the loading capacity (and losses) to these variables. Target values for the [Al]/[F] ratio were 2.0 and 1.5. After observations of relatively high capacity (or low losses) on the initial two experiments (Cr315 and Cr316), the third experiment was targeted for 7.0 M total [NO_3^-] and an [Al]/[F] molar ratio of 1.5. Unfortunately, the data for Cr317 clearly show that more raffinate volume was collected than expected (1348 mL vs 1202 mL) and the feed analyses showed that both the acid and total nitrate were 1 to 1.5 M higher than planned (see Tables 7 and 8). Three separate additions of 15.7 M HNO_3 were planned for the preparation of this feed solution. As a possible explanation for the acid concentration and volume discrepancy, it has been

[20] B. M Williamson, "Nuclear Criticality Safety Evaluation (NCSE): Dissolution of Plutonium (Pu) Metal", N-NCS-H-00276, Rev. 0, Savannah river Nuclear Solutions, LLC, Aiken, SC, May 2012.

suggested that the last 175-mL addition of 15.7 M HNO_3 would have accounted for this problem if it had been mistakenly added twice.

Flow Rates: Targeted and measured solution flowrates for column tests Cr315, Cr316, and Cr317 are provided in Table 9. The flow rates were determined from the volume of solution collected in each bottle and the recorded collection times. The average flow rate in each test for the column loading period with AFS-2 feed simulant was within 15% of the target value. The flow rates for the displacement step in each experiment were 16-25% lower than the target. As a result, only 52-58 mL of solution was collected in these bottles. Measured flow rates during the collection of hearts and tails solutions during elution were within 10% of the target values.

Material Balance: All solution that passed through the column was collected over a period of time and analyzed as a series of composite samples. Grab samples were also pulled after each 250mL of raffinate exited the column. Plutonium was included in the feed matrix[1, 4, 12] for each experiment based on the nominal flowsheet. ^{241}Am is a daughter product of ^{241}Pu for weapons grade material and thus is always present in a measurable amount in the feed to Pu anion exchange. A material balance was calculated for each experiment for Pu and ^{241}Am using the measured volumes of each sample from the raffinate, wash and elution steps (Tables 10a, 10b and 10c). Analytical results for ^{241}Am were not corrected to the time of separation.

Separately, the volume associated with each spectrum was calculated so that the appearance of the raffinate could be correlated to the amount of solution that had been pumped through the column. Later, when models allowed prediction of the Pu concentration for the set of spectra, a cumulative material balance showing cumulative Pu loading and losses could then be calculated as a function of feed and wash volume.

Americium is generally reported as being separated by anion exchange from Pu, but it was observed in previous work[4] that there appears to be some slight retention by the resin. Americium was observed in the spectra of the raffinate about the same time as the Fe appeared, but the small peak associated with Am (at ~510 nm) appears to slowly grow during continued loading and then shrinks during the wash step and a 5.8 BV wash appears capable of removing > 98% (DF > 72) of the Am (see Tables 10a, 10b and 10c). The gradual growth of the peak in the raffinate solution during continued loading appears to be the results of chromatographic separation of Am due to a small Kd for the resin.

Spectral Observations – Cr315: Spectra collected during the loading and wash cycles for Experiment Cr315 are provided in Figures 10a through 10e. All spectra are plotted as absorbance (y-axis) vs. wavelength in nm (x-axis). The lower spectrum in each figure includes the second derivative of the absorbance. The second derivative plots tend to minimize baseline drift effects making it easier to compare the spectra in a given series. The same general color coding was used for all spectral plots, with blue representing initial spectra, green being used for intermediate spectra, and red being used for later spectra in a given series. The spectra recorded during the first portion of Experiment Cr315, during the processing of the first 1.0 liters (11.8 BV) of feed through the column, are provided in Figure 10a. During this processing period the first four grab samples (EG1 through EG4) were collected. The trends observed in these early spectra were similar to those observed in subsequent experiments. An Fe peak centered near 410 nm was observed to grow with time followed by a small Am peak centered near 510 nm. The apparent decrease in the intensity of the Fe peak near the end of this time period is not understood since this peak is typically observed to reach a maximum midway through column loading. The Am peak continued to gradually increase with time as the solution volume was processed. An expanded view of these spectra is provided in Figure 10b.

Cr315 was unique from the other column experiments conducted in that some Pu^{3+} was observed to exit the column during the period between the end of the loading phase and the beginning of the wash phase. As shown in Figure 10c, a small amount of trivalent Pu was observed in the raffinate during this period as indicated by absorption bands near 565, 605, and 660 nm. This processing period corresponded to the time when the last 180 mL of feed and the first 150 mL of wash were pumped through the column. Since no Pu^{3+} standards were included in the models, the total Pu would not be expected to be predicted accurately by the Pu^{4+} models in the region. The spectrum collected near the end of the column wash which was dominated by Pu^{4+} absorption is also provided in the lower, second derivative plot in Figure 10c for comparison. It is speculated that a very small amount of reductant was somehow introduced into the column during this time which led to the reduction of some Pu^{4+} to Pu^{3+} and the subsequent loss of this material from the column. There were not any actions to which we have been able to attribute as the cause of this reduction. The amount of Pu lost due to reduction is small relative to the total amount loaded (based on the known molar absorptivity[21] for Pu^{3+}) and the effect on the column loading performance evaluations is believed to be minimal. As shown in Figure 10d and Figure 10e, increasingly more Pu^{4+} is observed to exit the column (absorption bands near 485, 535, 610, 650, and 685 nm) toward the end of the loading phase and during the wash phase.

Spectral Observations – Cr316: As shown in Figure 11a through Figure 11e, similar trends were observed in the spectra recorded for Experiment Cr316 as were observed for Cr315, except that no Pu^{3+} was observed. An overview of spectra collected during the entire column loading and wash phases is provided in Figure 11a, where Fe, Am, and Pu^{4+} breakthrough are sequentially observed in the raffinate and wash solutions. Note that the Fe absorption band is not clearly seen in this figure due to the fact that the lower wavelength range plotted is only 450 nm. The wavelength range for this plot was selected to emphasize the break-through of Am and Pu from the column. In Figure 11b the spectra recorded for the column loading phase during the processing of the first 250 mL (2.9 BV) of feed are provided. These spectra clearly show the gradual increase in the Fe absorption band since the lower wavelength range plotted is 350 nm. Interestingly, the iron absorption band is shifted to a slightly lower wavelength (centered near 395 nm) than was observed for Cr315. Americium is also observed near 510 nm for the later spectra. The growth of the Am peak during the processing of the last liter of feed solution (cumulative volume range from 250 to 1159 mL) is shown in Figure 11c. Finally, the loss of Pu^{4+} from the column following the loading phase and during column washing is shown in Figure 11d. Very little Pu breakthrough was observed for this experiment during column loading.

Spectral Observations – Cr317: Spectral results for Experiment Cr317 are provided in Figure 12a through Figure 12c. An overview of spectra collected during the entire column loading and wash phases is provided in Figure 12a, where Am and Pu^{4+} breakthrough are sequentially observed in the raffinate and wash solutions (Fe absorption band near 400 nm not shown). Spectra recorded while processing the first 1303 mL (15.2 BV) of feed solution are provided in Figure 12b. This time period covers nearly all of the loading phase of the experiment (total feed processed was 1348 mL). As a result of the fact that the Fe absorption peak was not shown and the fact that little Pu breakthrough occurred during this period, the Am peak near 510 nm is the dominant peak observed. Initial Pu^{4+} breakthrough is observed in the last few spectra shown in red. Spectra recorded during the last portion of the loading phase and through the wash phase are provided in Figure 12c. Peaks associated with Pu^{4+} are clearly the dominant peaks observed in this series of spectra.

Modeling Results: Multiple models were developed using various combinations of standard spectra. Those models generally agreed to within +/- 20% for Pu concentrations of greater than 0.1 g/L. It had

[21] *The Chemistry of the Actinide Elements*, J. J. Katz, G. T. Seaborg, L. R. Morss, 2nd Ed., Chapman and Hall, New York, 1986, Vol. 1, p 787.

been intended to minimize the uncertainty in the Pu standards by accurately measuring the stock calibration solutions in triplicate but due to sample preparation issues, these calibration solutions had higher than desired uncertainties of 4-7 % rather than ~1% as desired (Table 4). This and other issues with the standard preparation limited the accuracy from modeling of the calibration data. A different model for each experiment was used to predict the Pu concentration of each set of spectra that was associated with raffinate as it exited from the column.

DISCUSSION AND APPLICATION

Fluoride Analysis: The F analysis results reported in Table 8 are inconsistent with the known KF reagent masses added to the feed solutions for each experiment. Fluoride analysis in this solution matrix has historically been problematic due to the observation of a double peak in the anion chromatography effluent for F that is not fully understood. The authors speculate that this problem may be due to speciation change after the sample is injected into the Ion Chromatography (IC) eluate stream as the low pH diluted sample mixes with the high pH eluate solution; however no testing has been performed to confirm this hypothesis. As a result, the calculated [Al]/[F] ratios for the three experiments differ significantly from the values calculated based on the reagent masses added (Table 7). Method refinement of the analytical method is needed to obtain accurate Fe analysis results for this solution matrix. As far as the current work is concerned, the mass values for KF and ANN are far more accurate than the solution analyses. Thus we are confident that the planned [Al]/[F] ratios for the feed solution were tested.

Loading Profiles: After calculation of the Pu concentration of the raffinate as observed in the raffinate spectra, a plot of the Pu losses as a function of feed/wash volume could be plotted. Figure 13 shows a plot of the Pu losses for the three experiments described in this report. The results from experiment Cr315 were complicated by the appearance of Pu^{3+} from an unidentified cause which resulted in unusual losses that were observed earlier than in the other experiments. Although the Pu^{3+} is not expected to be predicted accurately by the models, it appears to cause an interference that bias' the Pu^{4+} predictions high. Also shown on Figure 13 is the cumulative resin loading for each of these experiments. Because the feed concentration is slightly different for each of the three experiments, it is difficult to directly compare the losses between these experiments. Previously this type of comparison[8] was performed by plotting the losses and loading against the grams of Pu fed to the resin column. In the previous loading study[8], a relatively short (12.7 cm) column of resin was used which had a much smaller residence time compared with the 68.8 cm column used in the current study. The current column is a full height column and this large resin volume results in a significant delay time between when the feed solution enters the bottom of the column and the raffinate leaves the resin bed. At any time during the column loading step there is a significant volume of Pu solution within the resin bed which has yet to contact unloaded resin. Therefore it is difficult to determine what loading to associate with the measured Pu concentration in the raffinate. The results are further complicated by the decision to stop loading after reaching a target of ~70 g Pu/L resin. While this loading is significantly higher than planned for the process, it meant that we did not get significant column breakthrough until after the wash step had begun. In other words, the wash step was started about the same time that the resin started to "leak" Pu from the bed.

To compensate for these difficulties, the results were plotted differently than in the previous study. The measured resin loading and raffinate losses were compared by plotting against an adjusted feed volume which reflects the equivalent volume of solution associated with a concentration of 5 g Pu/L (see Eq. 8). When the data is plotted this way the resin loading plots (Figure 14) fold into a single line, with the resin loading value dropping once the wash step was started. The Pu raffinate losses in g Pu/L can now be directly compared between the different experiments. Figure 14 suggests that as

the resin loading approaches 1400 adjusted mL (80 g Pu/L resin loading) that the incremental Pu losses will approach 10% of the feed concentration.

$$(8)\quad V^{*}(adjusted) = V(experimental) * \frac{[Pu]_{feed},\ M * 239\ g\ Pu/mol}{5\ g\ Pu/L}$$

Figures 15 and 16 are similar plots for the cumulative losses for both actual volume and adjusted volume. Because of the Pu^{3+} appearance, Cr315 shows an early breakthrough but again the appearance of Pu^{3+} is not expected in the plant process. Considering the uncertainties, the results from these three experiments are not much different from each other. Interpretation of the expected losses at various loadings was more difficult than anticipated due to the delay caused by the solution hold-up within the resin bed of a full-height column. It is apparent that in the 70 to 75 g Pu/L resin loading range that the resin column starts to lose significant Pu. Almost all of the losses were observed during the 5.8 BV wash step. The losses for these three experiments were 3.5 to 6.5% of the feed for loadings in the 69 to 76 g Pu/L resin range. Losses would have continued to accumulate if a full 10 BV of wash solution were used. For comparison, the two Pu tests performed during the DF testing[4] had resin loading in the 64-69 g Pu/L resin range. These tests had minimal losses during the load step (< 0.03%) but had 1.1 to 1.4% Pu losses during the 10 BV wash step. The bulk of those losses occurred during the last 5 BV of the 10-BV wash step.

Displacement and tails cut losses were in addition to those losses but will be highly dependent on implementation in the field. Although displacement and tails cut losses were observed in the 2-5% range for the current study, no effort was made to optimize those cuts. The authors judge that with the use of existing instrumentation (spectrophotometer or colorimeter) in HB-Line, it should be possible to reduce the displacement and tails losses to < 1% total in both the laboratory and field settings. Smith[12] assumed an anion exchange efficiency of 95% for the conversion to precipitation feed, which appears to be reasonable.

Disclaimer: This report involves the analysis of many individual data points, all of which have uncertainties in the 5 to 30% range. Although efforts were made to reduce the uncertainty in measurements that were recognized as critical, there are a number of examples where the measurement uncertainty appears to limit the result. Also the duration of this study did not allow any experiments to be repeated, so the reproducibility of these results could not be confirmed. Recommendations on the resin loading levels expected to give acceptable product losses are based on testing conducted under ambient laboratory conditions (18-23 °C). Increased losses for a given resin loading could occur at higher processing temperatures. The effect of aging of the resin was not tested in this study but based on previous studies, it is considered likely that resin capacity will not be seriously reduced until after a relatively significant amount of processing has been performed.

RECOMMENDATIONS

Further Work: The following are recommendations to address the recognized limitations of the work performed thus far.

- The processing of calibration data into models involves many steps and the use of the DOS-based MVA program has many limitations. Porting the MVA program capability into Microsoft Excel macros would greatly simplify the model development process and reduce the effort required to perform similar work in the future.
- The lower practical range of total [NO_3^-] and [Al]/[F] molar ratio was not identified in this work. Additional experiments should be performed to investigate if a total [NO_3^-] of 7 M would yield acceptable Pu loading performance (i.e. low Pu losses at a similar resin loading). At the same time lower molar ratios of [Al]/[F] should also be investigated to expand the range of acceptable operating conditions.
- The exclusive use of a full height (27 inch/68.8 cm) resin bed limited the interpretation of the loading data. Additional testing with a short test bed for future loading studies should be considered. The use of both a short bed and a full height bed would likely generate a better understanding of the effect that variation in the feed solution has on resin capacity.
- This study was limited by the uncertainties associated with the differences between the compositions of the feed solution for each experiment. Further work should take every effort to reduce these uncertainties. It is very important to make up the feed solutions consistently to avoid undesired compositional differences. Solution analyses are generally not precise enough to characterize the differences between the various feed solutions as a typical 10% uncertainty is relatively large compared to the differences being tested.
- Development of the Anion Chromatography analytical method is needed to obtain accurate fluoride analysis results for the solution matrices of interest to this work. These analytical difficulties should also be considered when developing the basis for validation of fluoride additions in the dissolution process. Inaccurate fluoride analyses may limit the ability to achieve the desired [Al]/[F] molar ratio target values.

CONCLUSIONS

These loading experiments show that a representative feed solution containing ~5 g Pu/L can be loaded onto Reillex™ HPQ resin from solutions containing 8 M total nitrate and 0.1 M KF provided that the F is complexed with Al to an [Al]/[F] molar ratio range of 1.5-2.0. Lower concentrations of total nitrate and [Al]/[F] molar ratios may still have acceptable performance but were not tested in this study. Loading and washing losses should be relatively low (<1%) for resin loading of up to 60 g Pu/L. Loading somewhat above this level is possible, but Pu wash losses will increase such that 10-20% of the additional Pu fed may not be retained by the resin.

APPENDIX: Figures and Tables

Table 1. PuO_2 Specification Limits.[1,2]

Chemical Component		B µg/g Pu	A µg/g Pu	Exceptional µg/g Pu
Ag	(Silver)	100	250	10,000
Al	(Aluminum)	100	500	10,000
Am	(Americium)		7000	
B	(Boron)	1	100	1000
Be	(Beryllium)	100	100	2000
Bi	(Bismuth)	10	100	1000
C	(Carbon)	500	1000	5000
Ca	(Calcium)	150	500	10,000
Cd	(Cadmium)	5	10	1000
Cl	(Chlorine)	250 [a]	250 [a]	500
Co	(Cobalt)	50	100	10,000
Cr	(Chromium)	200	1000	1500
Cu	(Copper)	100	100	500
Dy	(Dysprosium)	0.5	1	1000
Eu	(Europium)	0.5	1	1000
F	(Fluorine)	250 [a]	250 [a]	350
Fe	(Iron)	500	2000	3000
Ga	(Gallium)	0.12	12,000	12,500
Gd	(Gadolinium)	0.5	3	250
In	(Indium)	20	20	1000
K	(Potassium)	100	300	10,000
Li	(Lithium)	100	400	10,000
Mg	(Magnesium)	200	500	10,000
Mn	(Manganese)	100	100	1000
Mo	(Molybdenum)	100	100	1000
N	(Nitrogen)	300	400	400
Na	(Sodium)	100	1000	10,000
Nb	(Niobium)	50	100	3500
Ni	(Nickel)	200	5000	12000
Np	(Neptunium)		500	
P	(Phosphorus)	250 [b]	200	1000
Pb	(Lead)	100	200	1000
S [b]	(Sulfur)	250 [b]	250	1000
Si	(Silicon)	150	200	200
Sm	(Samarium)	2	2	1000
Sn	(Tin)	100	100	2500
Ta	(Tantalum)	200	200	500
Th	(Thorium)	50	100	100
Ti	(Titanium)	100	100	2500
U	(Uranium)	100	5000	
V	(Vanadium)	5	300	2500
W	(Tungsten)	100	200	2500
Zn	(Zinc)	100	150	1000
Zr	(Zirconium)	50	50	1000

[a] Limits for F and Cl are F+Cl < 250 for Column A.

[b] Limits for P and S are P+S < 250 for Column B.

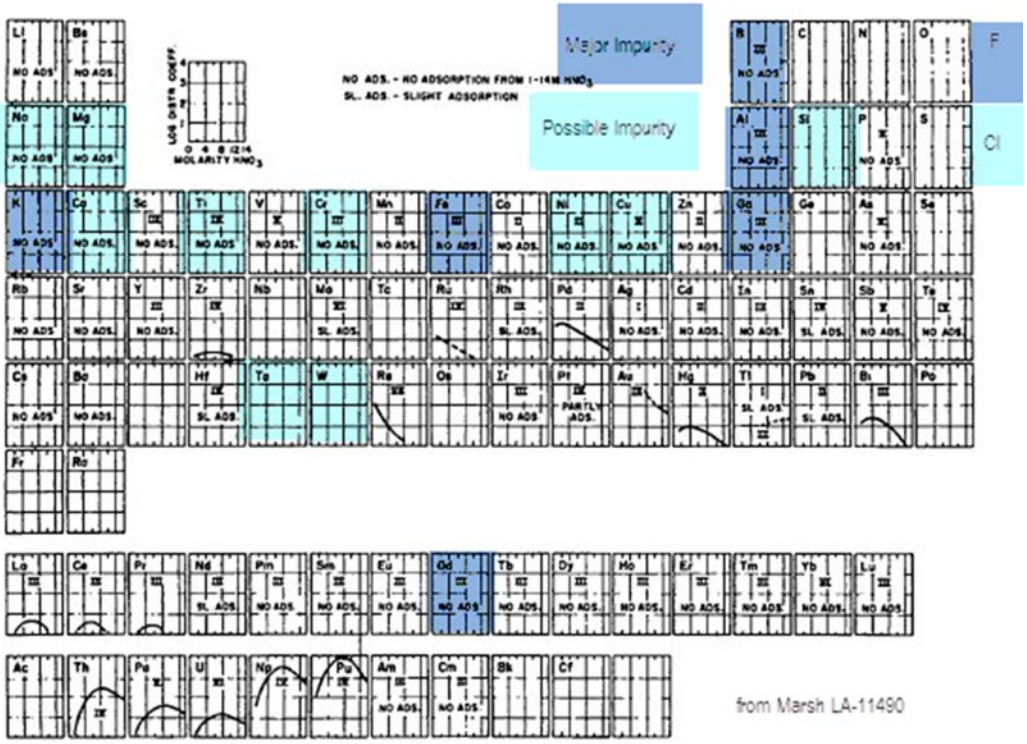

Figure 1. Distribution Coefficients in a Nitrate Anion Exchange System with Expected Impurities in HB-Line Process.

Table 2. Process Scaling: HB-Line Column vs SRNL Ce and Pu Columns.

			Recon-ditioning	Feed	Decontamination initial	Decontamination final	Elution		
		Pu (g/batch)		1200					
		Pu (g/l)		4.5					
		HNO3 (M)	8	8	8	8	0.35		
294.2	cm^2	HB-Line	up	up	up	up	down		
68.58	cm	Flow (L/min)	1.4	1.1	1.1	2	0.7		
		v (mL/min/cm^2)	4.8	3.7	3.7	6.8	2.4		
20.2	L	Volume (L)	30	260	40	160	60		
		Time (min)	21	236	36	80	86	7.7	h total
		BV	1.5	13.0	2.0	8.0	3.0		
		mgs Pu/min/cm^2		17					
2.835	cm^2	SRNL Hood -Ce	up	up	up	up	down		
68.58	cm	Flow (mL/min)	20	10.6	10.6	19.3	6.8		
1.90	cm	v (mL/min/cm^2)	7.1	3.7	3.7	6.8	2.4		
194.44	cc	Volume (mL)	200	1964	388	3492	450		
		Time (min)	10	185	37	181	66	8.0	h total
		BV	1.0	10.1	2.0	18.0	2.3		
		mgs Pu/min/cm^2		19					
1.247	cm^2	SRNL Glovebox -Pu	up	up	up	up	down		
68.58	cm	Flow (mL/min)	10	4.5	4.5	8.5	3		
1.26	cm	v (mL/min/cm^2)	8.0	3.6	3.6	6.8	2.4		
85.512	cc	Volume (mL)	100	1000	172	688	260		
		Time (min)	10	222	38	81	87	7.3	h total
		BV	1.2	11.7	2.0	8.0	3.0		
		mgs Pu/min/cm^2		18					

Note: Up and down designates flow direction through resin bed

Figure 2a. Screen used to Retain Resin Bed.

The position of the two column segments was reversed upon installation in the glovebox (from that shown above. Left and Right designations in the text are in reference to this figure not to the actual equipment.

Figure 2b. Assembled Column for Glovebox Pu Experiments.

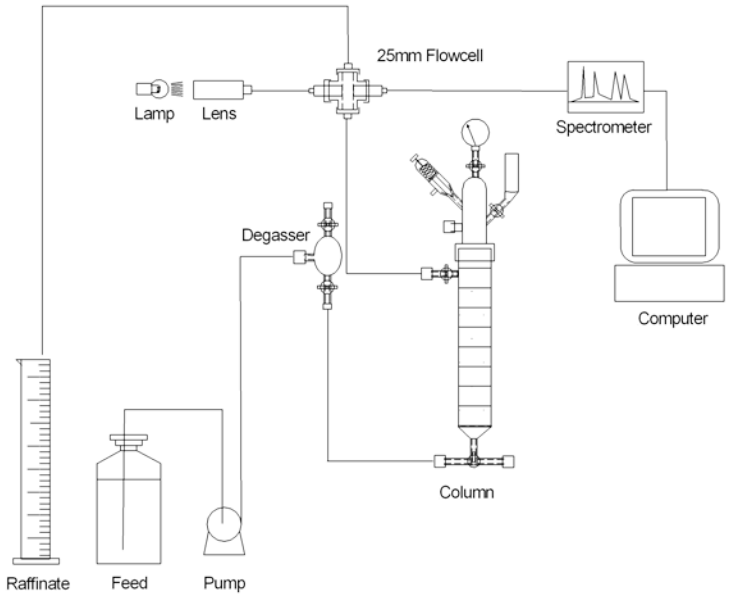

Figure 3. Up-flow Load/Wash Experimental Setup.

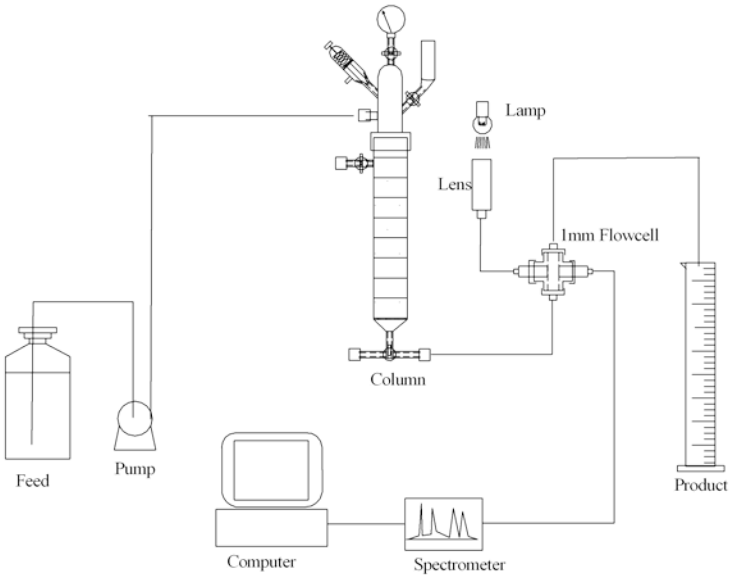

Figure 4. Elution Experimental Setup.

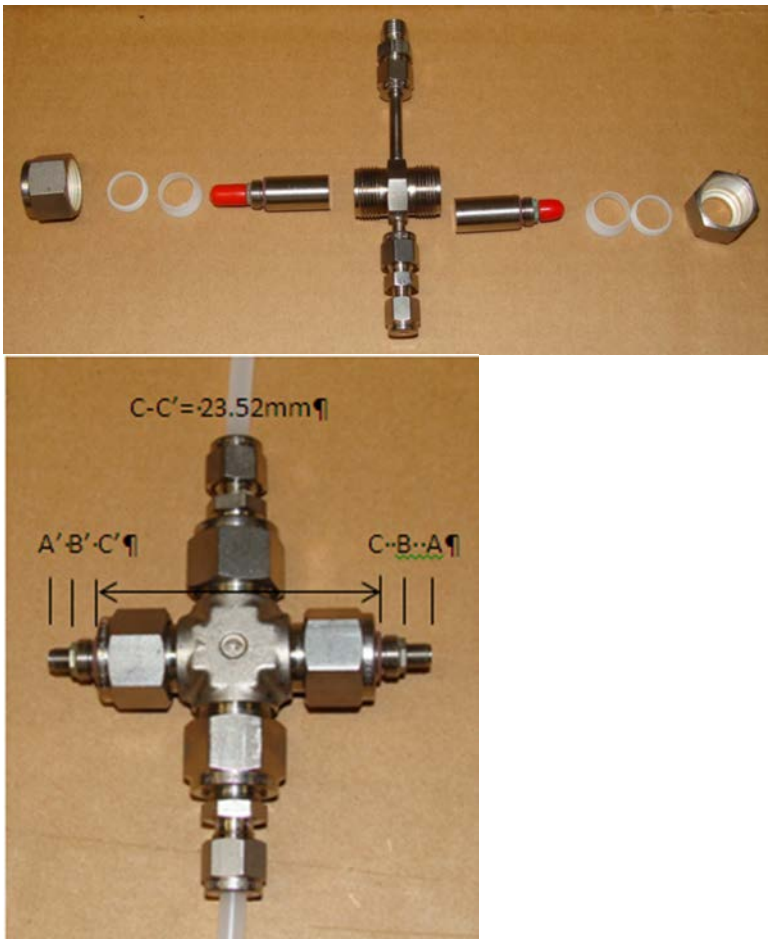

Figure 5. Effluent Stream Flowcell.

Table 3. Spectrophotometer System Parts List.

- Spectrometer: Thermo-Electric Cooled Fiber Optic Spectrometer, 75 mm Avabench, 2048 pixel TE cooled and regulated CCD detector, with a >150 nm Deep UV detector coating, 25 µm slit size, sorting coating with 350 and 590nm longpass filter for UA grating, wavelength range 200-1,100 nm using a USB2 high speed interface to a laptop computer operating Windows XP
- Fiber optic cable: Ceramoptec or Polymicro, 400 micron high-OH core with SMA fittings each end
- Flowcell: Swaglock ½ " Union Cross (SS-810-4) for body, Swaglock ¼" to ½ " Reducer (SS-400-R-2) 2 each to attach ¼" poly tubing, Fiber optic Lens: Equitech CL-UV-K. Stainless steel body, 1/2" diameter. Quartz lens. Kalrez o-ring seal. Stainless SMA connector, 2 required
- Light Source: Ocean Optics Tungsten Halogen LampHousing, LS-1
- Variable Attentuator Oz Optics Part # BB-200-55-300 600-SP to adjust light levels
- Cuvette Blocks: SRNL fabricated plexiglass cuvette holders each with 2 lenses similar to flowcell

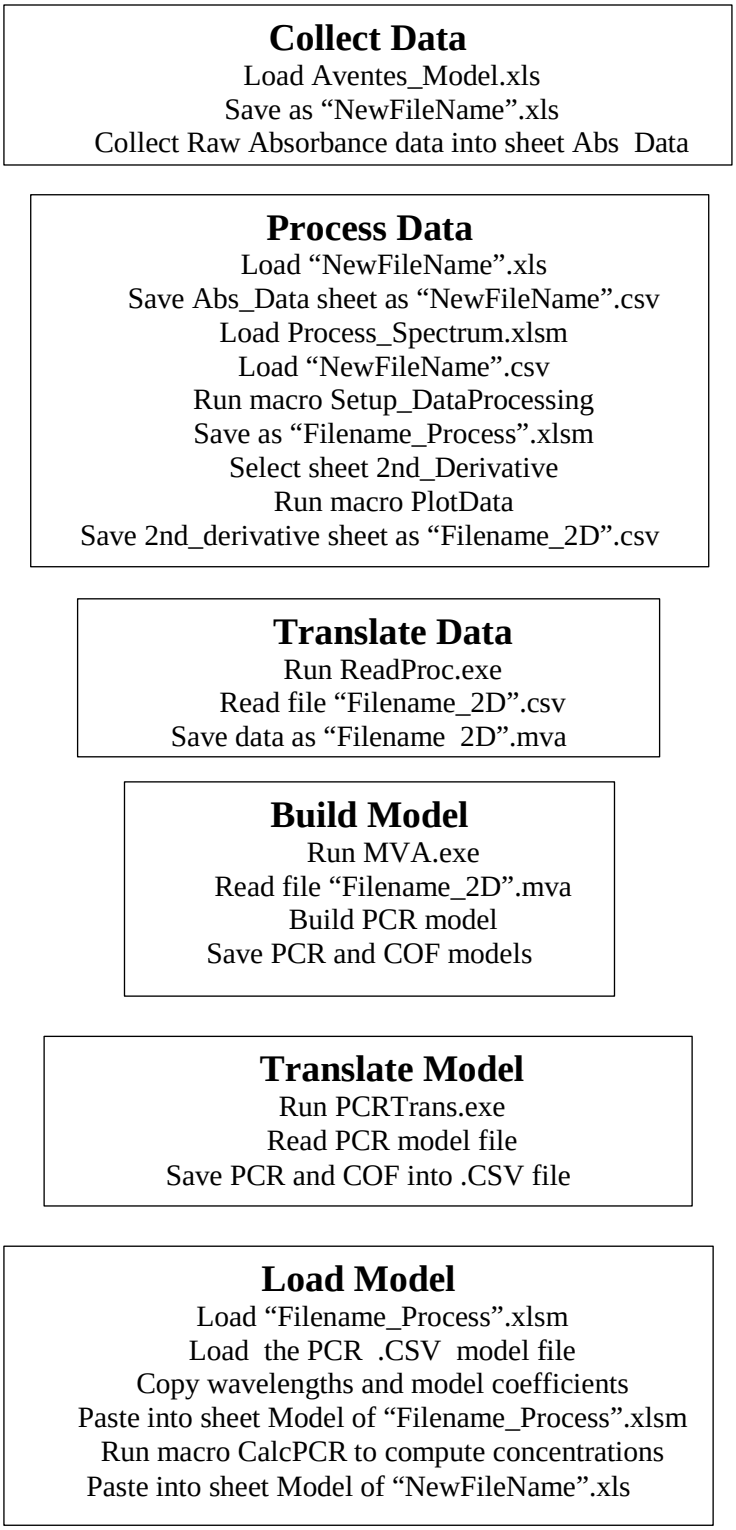

Figure 6. MVA Modeling Flow Diagram.

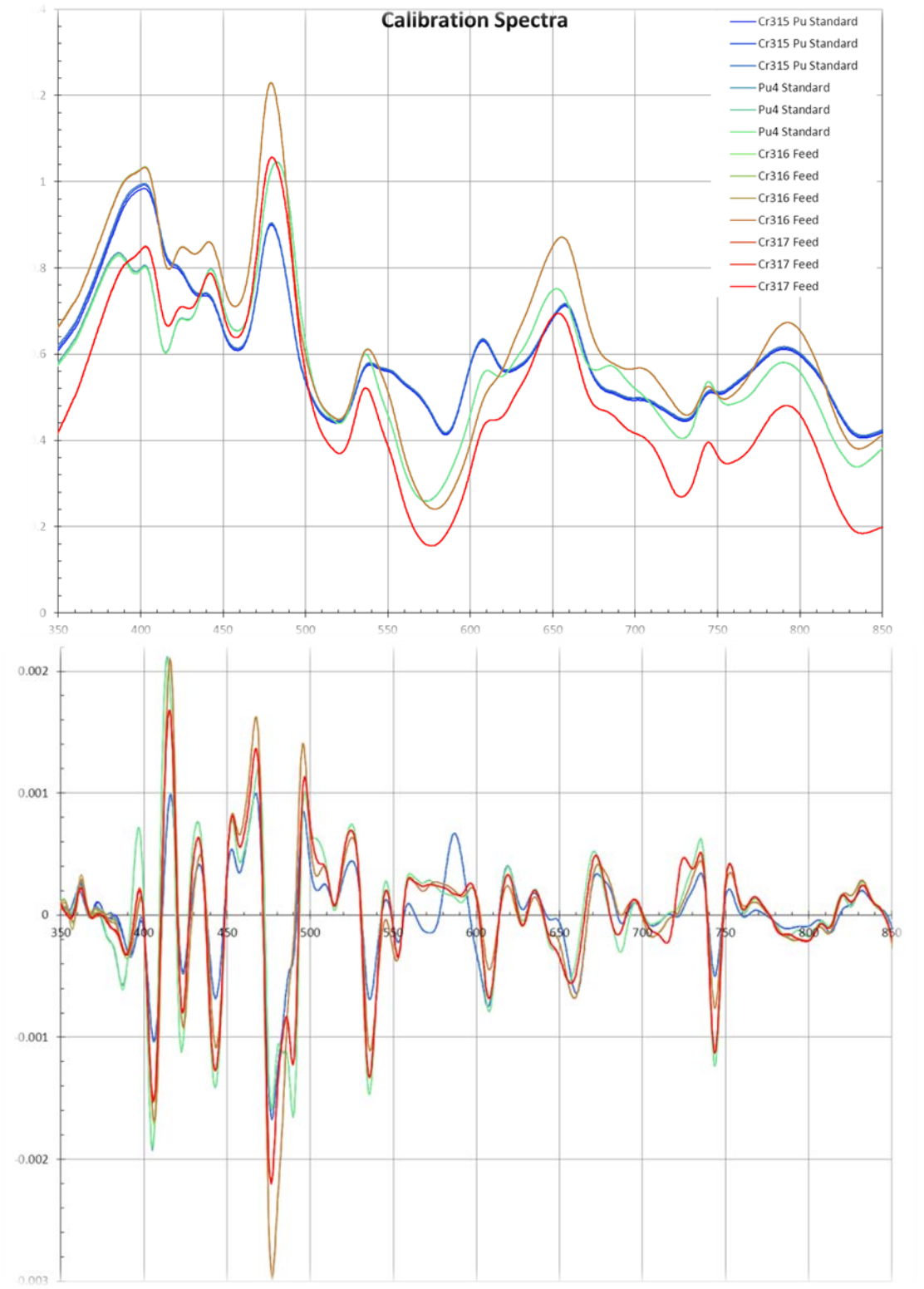

Note: Color varies with time starting with Blue for the initial spectra, changes to Green and ends with Red for all graphs unless otherwise noted. Unlabeled X-axis on spectra plots are in Wavelength, nm. Unlabeled Y-axis on spectra plots are absorbance on upper plots and 2nd deriviative of absorbance on lower plot

Figure 7. Spectra of Calibration Solutions

Table 4. Calibration Solutions.

	Pu		NO_3	Al	F	Fe	$B(OH)_3$	H_2O_2	Pu Analysis	
Description	g/L	mM	M	mM	mM	mM	mM	mM	g/L	% RSD
Pu Spectra 8M	4.35	18.2	7.93					0.040	3.88	5.01%
Pu Std A	0.870	3.6	7.99					0.008		
Pu Std B	0.207	0.9	8.00					0.002		
Pu Std C	0.085	0.4	8.00					0.001		
Pu Std D	0.035	0.1	8.00					0.0003		
Cr315 Pu Spectra	4.35	18.2	7.89	199	100	58	114		3.99	4.89%
Cr315 Std A	0.870	3.6	7.89	199	98	58	114			
Cr315 Std B	0.207	0.9	7.89	200	98	58	114			
Cr315 Std C	0.085	0.4	7.89	200	98	58	115			
Cr315 Std D	0.035	0.1	7.89	200	98	58	115			
Cr316 Feed	4.36	18.3	7.90	149	100	58	114		5.33	4.50%
Cr316 Std A	0.872	3.7	7.79	149	100	58	114			
Cr316 Std B	0.208	0.9	7.77	149	100	58	114			
Cr316 Std C	0.086	0.4	7.76	149	100	58	114			
Cr316 Std D	0.035	0.1	7.76	149	100	58	114			
Cr317 Feed	4.43	18.6	6.94	150	102	44	115		5.01	6.86%
Cr317 Std A	0.887	3.7	7.42	161	20	47	123			
Cr317 Std B	0.211	0.9	7.51	163	5	47	125			
Cr317 Std C	0.087	0.4	7.53	163	2	47	125			
Cr317 Std D	0.035	0.1	7.53	163	1	47	125			

Table 5. Preparation of Stock Solutions for Spectra Reference Solutions.

Description	Pu		HNO_3	F	Al	Gd	$B(OH)_3$
	g/L	mM	M	mM	mM	mM	mM
Cr259PC1	59.58	249	1				
2.0M KF in 8M HNO_3	0		8.0	1997			
0.251M $B(OH)_3$ in 8M HNO_3	0		8.0				251
0.053M Gd in 8M HNO_3	0		8.0			53.2	
0.6M Al in 8M HNO_3	0		8.0		0.604		
8M HNO_3	0		8.0				

Table 6. Composition of Spectra Reference Solutions.

Description	Pu		HNO_3	F	Al	Gd	$B(OH)_3$
	g/L	mM	M	mM	mM	mM	mM
Pu	4.47	18.7	8.06				
Pu 0.05M KF 0.2 g/L Gd	4.47	18.7	8.06	50		1.33	
Pu 0.05M KF 0.2 g/L Gd 0.015 M Al	4.47	18.7	8.06	50	15	1.33	
Pu 0.05M KF 0.2 g/L Gd 0.030 M Al	4.47	18.7	8.06	50	30	1.33	
Pu 0.05M KF 0.2 g/L Gd 0.045 M Al	4.47	18.7	8.06	50	45	1.33	
Pu 0.05M KF 0.2 g/L Gd 0.1 M Al	4.47	18.7	8.06	50	106	1.33	
Pu 0.1M KF	4.47	18.7	8.06	100			
Pu 0.2M KF	4.47	18.7	8.06	200			
Pu 0.4M KF	4.47	18.7	8.06	399			
Pu 0.8M KF	4.47	18.7	8.06	799			
Pu 0.1M KF 1 g/L $B(OH)_3$	4.47	18.7	8.06	100			94
Pu 0.2M KF 1 g/L $B(OH)_3$	4.47	18.7	8.06	200			94

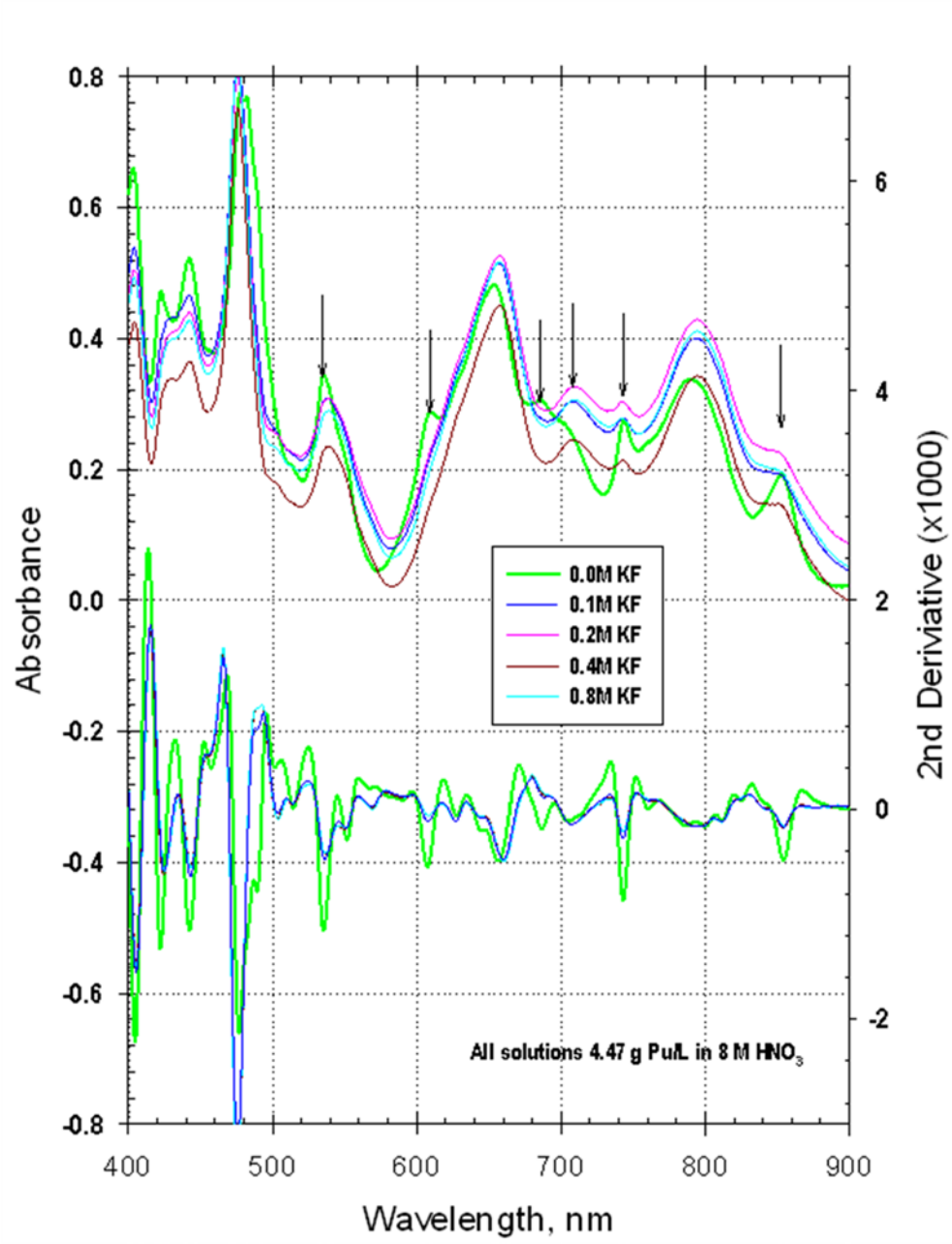

Figure 8. Effect of F on Pu Spectra.

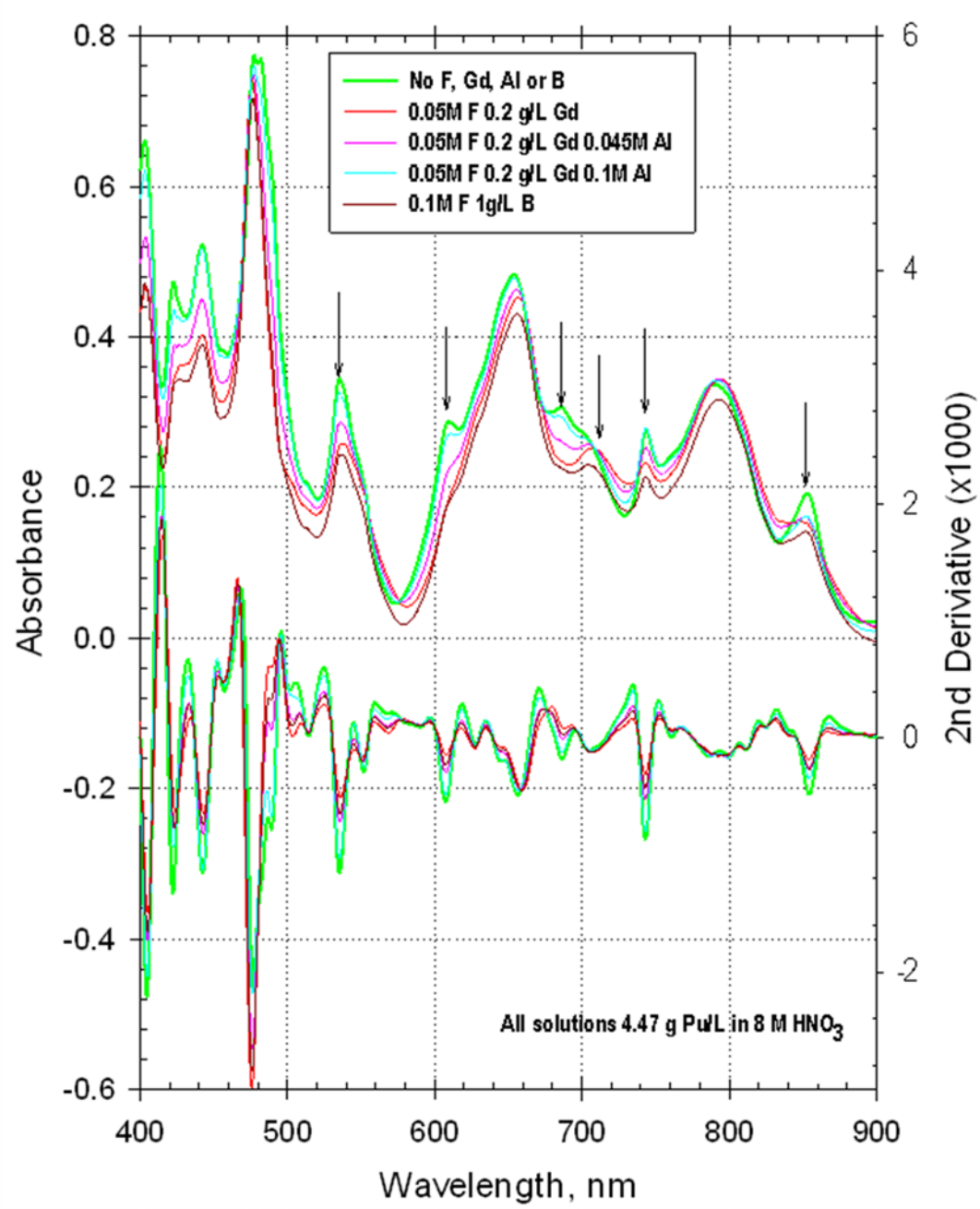

Figure 9. Effect of Gd, B and Al on Pu-F Complexation.

Table 7. Feed Preparation for Cr315, Cr316 and Cr317 Experiments.

Component	Cr315 Mass g	Volume mL	Cr316 Mass g	Volume mL	Cr317 Mass g	Volume mL
H_2O		300		299		485
KF	7.03		7.02		7.12	
$Al(NO_3)_3*9H_2O$	90.09		67.53		67.53	
$B(OH)_3$	8.50		8.51		8.53	
$Fe(NO_3)_3*9H_2O$	4.00		4.02		11.50	
40 wt % FS		25		25		10
Dissolved Pu in Nitric[a]		390		310		220
70 wt% HNO_3		450		461		375
40 wt% HNO_3		0		79		79
Water from reagents		40.3		31		33
Approx. Volume, mL		1205.3		1204.6		1202.2
Al:F mole ratio	2.05		1.54		1.53	
Total NO_3 (M)	7.91		7.90		6.93	
HNO_3 (M)	7.29		7.43		6.42	
Pu (g/L)	4.37		4.36		4.44	

[a] Pu solutions contained 3.5-5.5 M HNO_3, ~0.01-0.02 M KF and 13-24 g/L Pu.

Table 8. Feed Analysis.

	Cr315			Cr316			Cr317		
Element	mg/L	mM	ug/g Pu	mg/L	mM	ug/g Pu	mg/L	mM	ug/g Pu
AD Sample ID	3-299169			3-299171			3-299173		
Pu	4923	21		5333	22		5010	21	
Am	5.9	0.02	1200	6.1	0.03	1200	6.1	0.03	1200
Al	4960	184	1008000	4270	158	801000	3910	145	780000
B	1050	97	213000	1290	119	242000	1220	113	244000
Fe	3390	61	689000	3050	55		2180	39	435000
K	3210	82	652000	3810	97	714000	3450	88	689000
S	4240	132	861000	3630	113	681000	1530	48	305000
F	3008	158	611000	2504	132	470000	2136	112	426000
Nitrate	494967	7984	100549000	494802	7981	92779000	500000	8065	99803000
Al:F mole ratio		1.2			1.2			1.3	
Total Acid (M)		7.9			7.9			8.3	
Free Acid (M)		7.1			7.3			7.8	

Table 9. Targeted and Actual Flowrates.

	Target mL/min	Cr-315 Actual mL/min	Cr-316 Actual mL/min	Cr-317 Actual mL/min
Raffinate EG1	4.5	4.9	4.8	4.6
Raffinate EG2	4.5	4.2	5.0	4.8
Raffinate EG3	4.5	4.5	4.9	5.0
Raffinate EG4	4.5	4.7	4.7	4.6
Raffinate EG5	4.5	4.0	4.2	4.8
Raffinate EG6	4.5			4.6
Avg. Loading	4.5	4.5	4.8	4.7
Wash 1	4.5	4.8	4.8	5.0
Wash 2	8.5	8.4	8.4	8.6
Displacement[a]	3.0	2.3	2.5	2.5
Hearts	3.0	3.2	3.0	3.0
Tails	3.0	3.1	3.1	3.1
Avg. Elution	3.0	2.9	2.9	2.9

[a] Displacement flowrates were consistently below the target because the liquid head above the column was equilibrating during this step.

Table 10a. Material Balance for Pu Column Experiment Cr315 (85.5cc Two Piece Column Reillex™ HPQ).

		Cumulative	Cum. Bed	Pu		Pu	Am241	
	AD	Volume	Volumes	Conc.	Btl	Loaded	Conc	Btl
Sample	No.	Processed (mL)	Processed	g/L	g	g	mg/L	ug
Feed	3-298157	0	0.0	5.095	6.037	0.000	5.225	6192
EG1	3-298158	250	2.9	0.0017	0.000		3.702	11.1
EG2	3-298159	503	5.9	0.011	0.000		6.696	6.7
EG3	3-298160	754	8.8	0.011	0.000		6.420	6.4
ECA	3-298162	754	8.8	0.011	0.0084	3.833	6.328	4771
EG4	3-298161	1005	11.8	0.009	0.000		4.818	4.8
EG5	3-298163	1185	13.9	0.036	0.000		6.236	6.2
ECB/WC	3-298164	1697	19.8	0.326	0.308	5.721	2.547	2402
Disp	3-298165	1749	20.5	0.724	0.038	5.683	0.228	11.9
Hearts	3-298166	1851	21.6	56.024	5.714	-0.031	0.683	69.6
Tails	3-298167	1961	22.9	5.379	0.592	-0.623	0.029	3.2
Mat'l Balance		g Pu (Hearts/Tails)	6.31	Total Recovery	6.66	g Pu	7293	ug Am
			104.5%		110.3%		117.8%	of Feed
Resin Pu Loading				Pu Losses			98.9%	rejected
	Feed	66.9	g/L resin	0.354	g Pu (EC, WC, Disp)		89	Am DF
	Hearts and Tails	73.8	g/L resin	5.9%				

Terminology: EGx are Effluent Grab samples, ECx are Effluent Composite bottle samples, WC is the wash composite bottle sample, Disp is the displacement cut at the beginning of elution, Hearts is the Pu product cut, Tails is the dilute cut after Hearts

Table 10b. Material Balance for Pu Column Experiment Cr316 (85.5cc Two Piece Column Reillex™ HPQ).

		Cumulative	Cum. Bed	Pu		Pu	Am241	
	AD	Volume	Volumes	Conc.	Btl	Loaded	Conc	Btl
Sample	No.	Processed (mL)	Processed	g/L	g	g	mg/L	ug
Feed	3-298324	0	0.0	5.333	6.181	0.000	1.987	2303
EG1	3-298325	250	2.9	0.003	0.000		6.249	62.5
EG2	3-298326	500	5.8	0.000	0.000		0.000	0.0
EG3	3-298327	760	8.9	0.000	0.000		6.643	13.3
EG4	3-298329	1011	11.8	0.001	0.000		6.643	13.3
ECA	3-298328	1011	11.8	0.014	0.014	5.378	4.884	4937.7
EG5	3-298330	1159	13.6	0.000	0.000		6.407	12.8
ECB/WC	3-298331	1680	19.6	0.261	0.174	5.993	2.350	1567.5
Disp	3-298332	1733	20.3	0.562	0.030	5.963	0.158	8.3
Hearts	3-298333	1843	21.6	52.920	5.821	0.142	0.751	82.6
Tails	3-298334	1943	22.7	0.974	0.097	0.045	0.009	0.9
Mat'l Balance		g Pu (Hearts/Tails)	5.92	Total Recovery	6.14	g Pu	6699	ug Am
			95.8%		99.3%		291%	of Feed
Resin Pu Loading				Pu Losses			98.8%	rejected
	Feed	70.1	g/L resin	0.218	g Pu (EC, WC, Disp)		82	Am DF
	Hearts and Tails	69.2	g/L resin	3.5%				

Table 10c. Material Balance for Pu Column Experiment Cr317 (85.5cc Two Piece Column Reillex™ HPQ).

		Cumulative	Cum. Bed	Pu		Pu	Am241	
	AD	Volume	Volumes	Conc.	Btl	Loaded	Conc	Btl
Sample	No.	Processed (mL)	Processed	g/L	g	g	mg/L	ug
Feed	3-298335	0	0.0	5.010	6.753	0.000	5.895	7946
EG1	3-298336	250	2.9	0.0007	0.000		3.203	32.0
EG2	3-298337	510	6.0	0.0065	0.000		6.197	12.4
EG3	3-298338	762	8.9	0.0024	0.000		6.210	12.4
ECA	3-298339	764	8.9	0.0024	0.002	3.826	4.149	3112
EG4	3-298340	1014	11.9	0.0039	0.000		6.328	12.7
EG5	3-298341	1266	14.8	0.0036	0.000		6.604	13.2
ECB/WC	3-298342	1945	22.7	0.3150	0.375	6.376	2.298	2736.4
Disp	3-298343	2003	23.4	1.1040	0.064	6.312	0.242	14.0
Hearts	3-298344	2105	24.6	61.8625	6.310	0.002	1.088	111.0
Tails	3-298345	2205	25.8	1.6369	0.164	-0.161	0.046	4.6
Mat'l Balance		g Pu (Hearts/Tails)	6.47	Total Recovery	6.91	g Pu	6060	ug Am
			95.9%		102.4%		76.3%	of Feed
Resin Pu Loading				Pu Losses			98.6%	Rejected
	Feed	74.6	g/L resin	0.441	g Pu (EC, WC, Disp)		72	Am DF
	Hearts and Tails	75.7	g/L resin	6.5%				

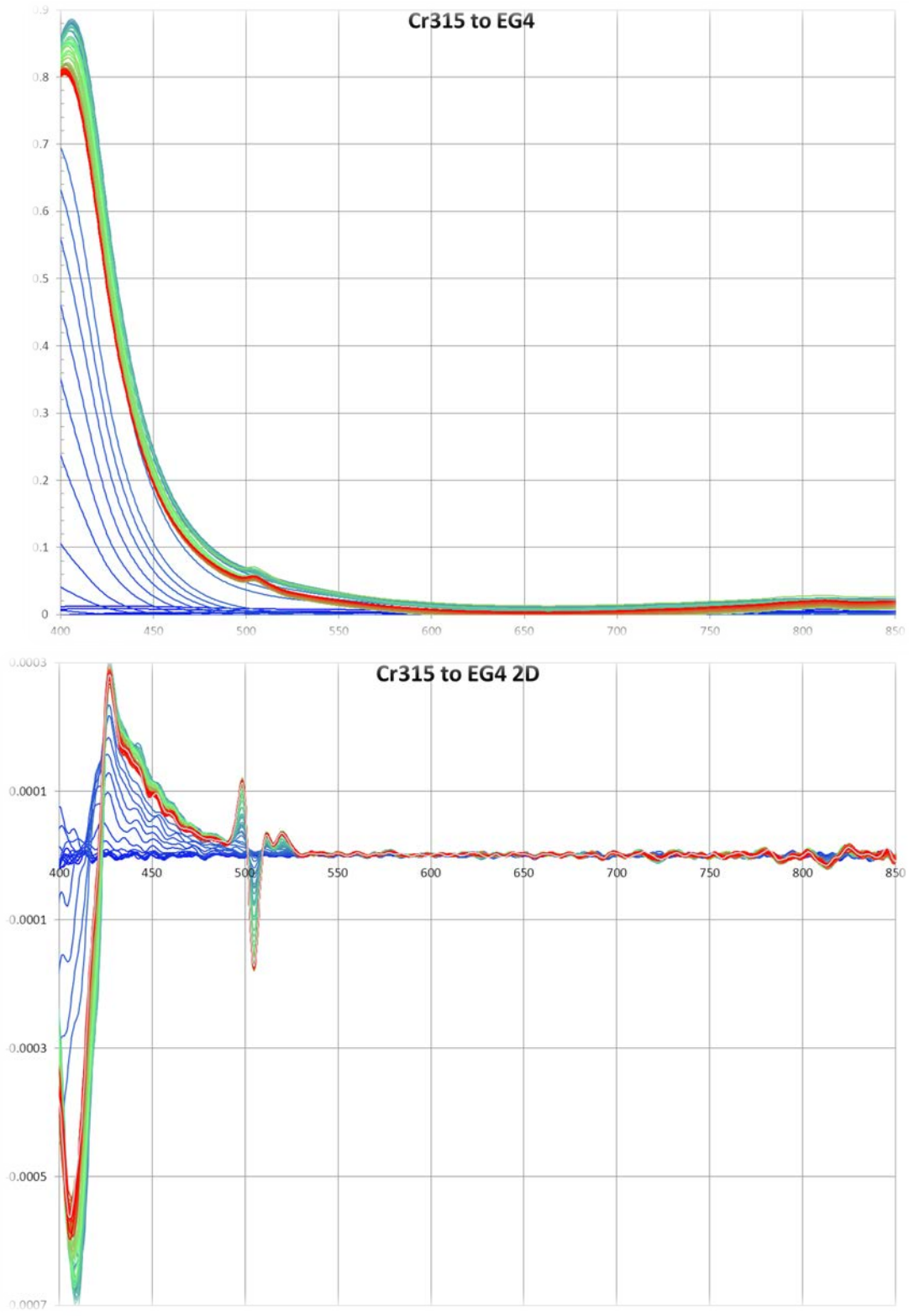

Figure 10a. Cr315 Spectra- Start to 1105 mL (11.8 BV).

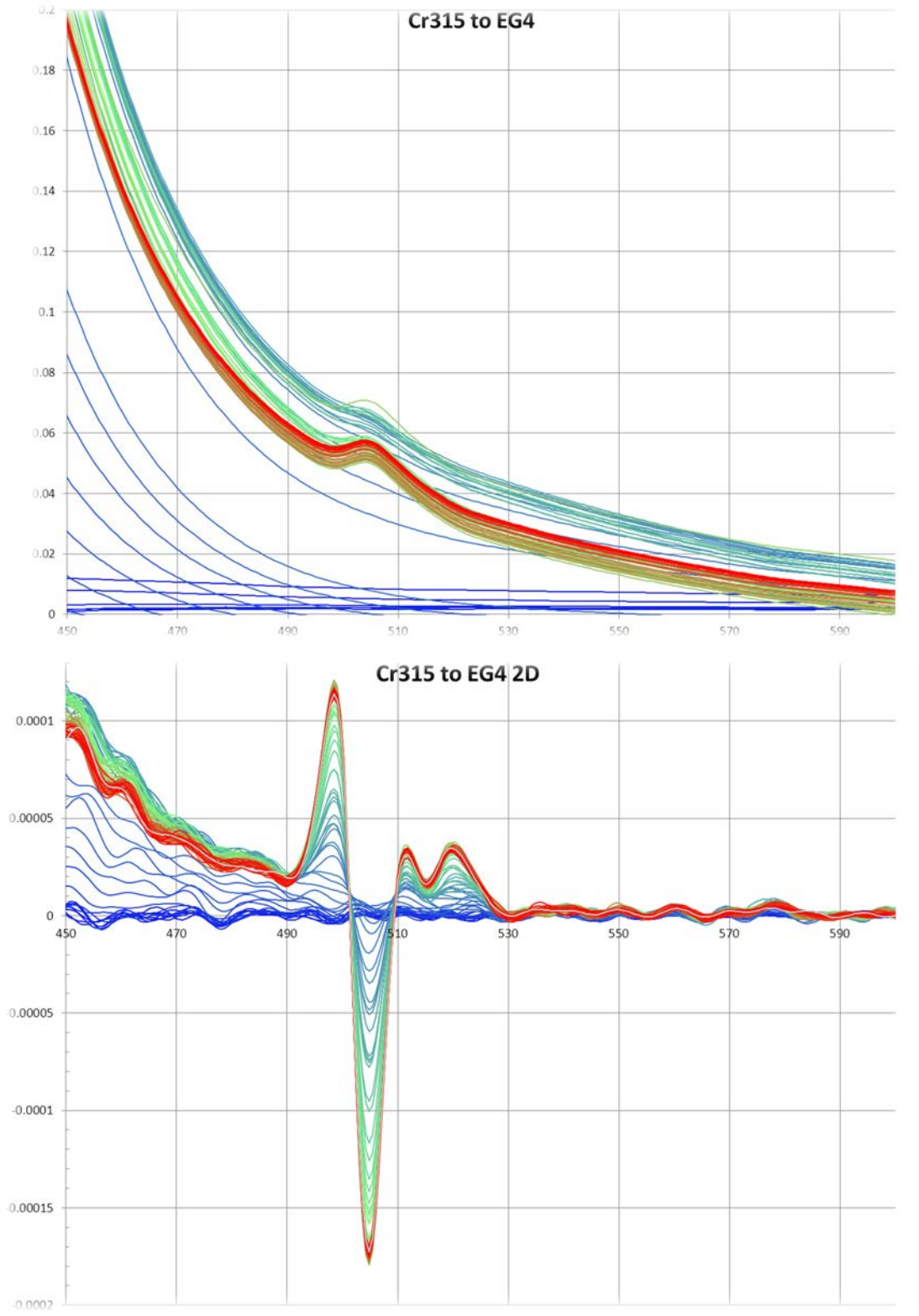

Figure 10b. Cr315 Spectra – Start to 1105 mL (11.8 BV), ^{241}Am Peak.

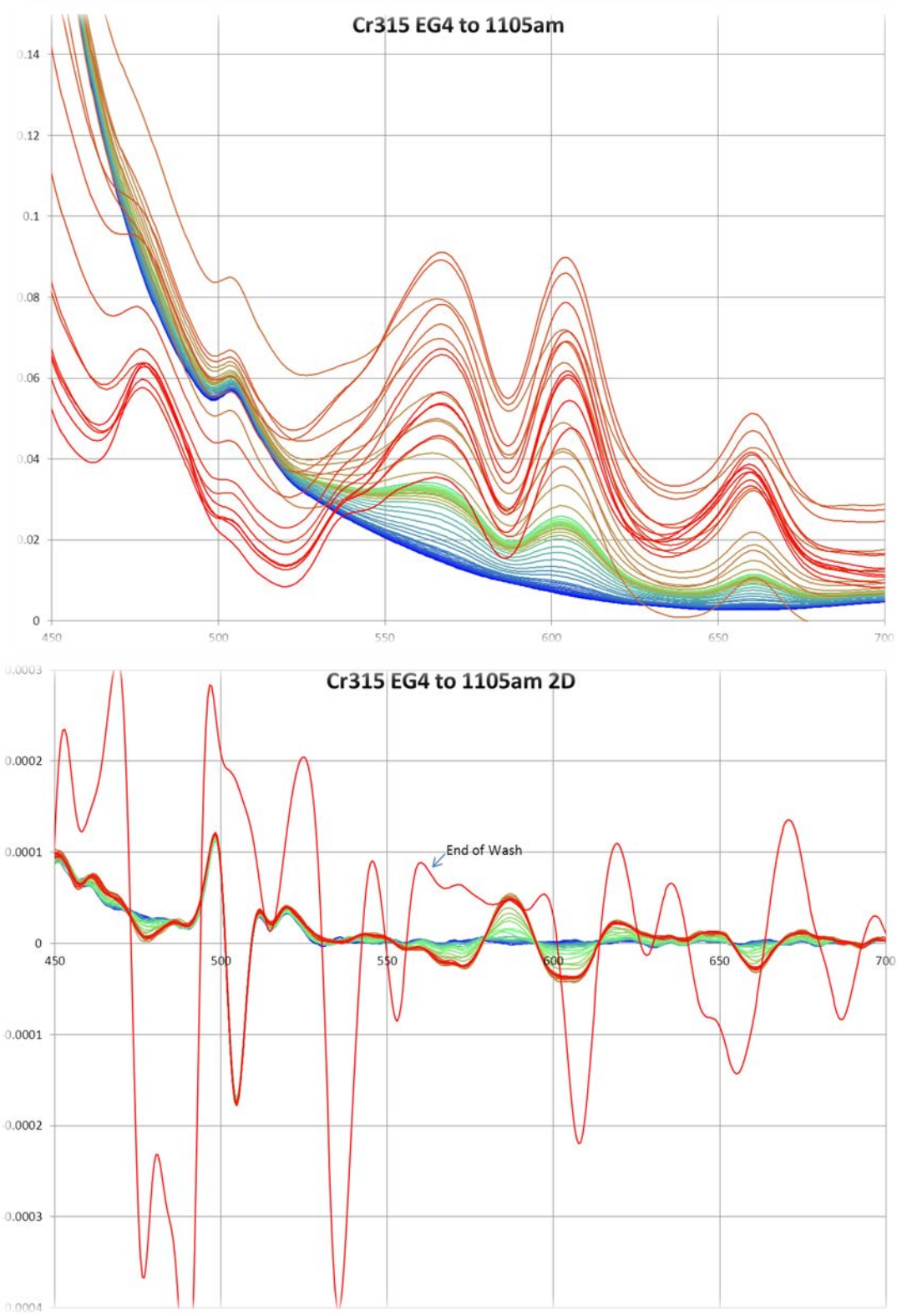

Figure 10c. Cr315 Spectra –1105 mL (11.8 BV) to 1332mL (15.6 BV), Appearance of Pu^{3+}.

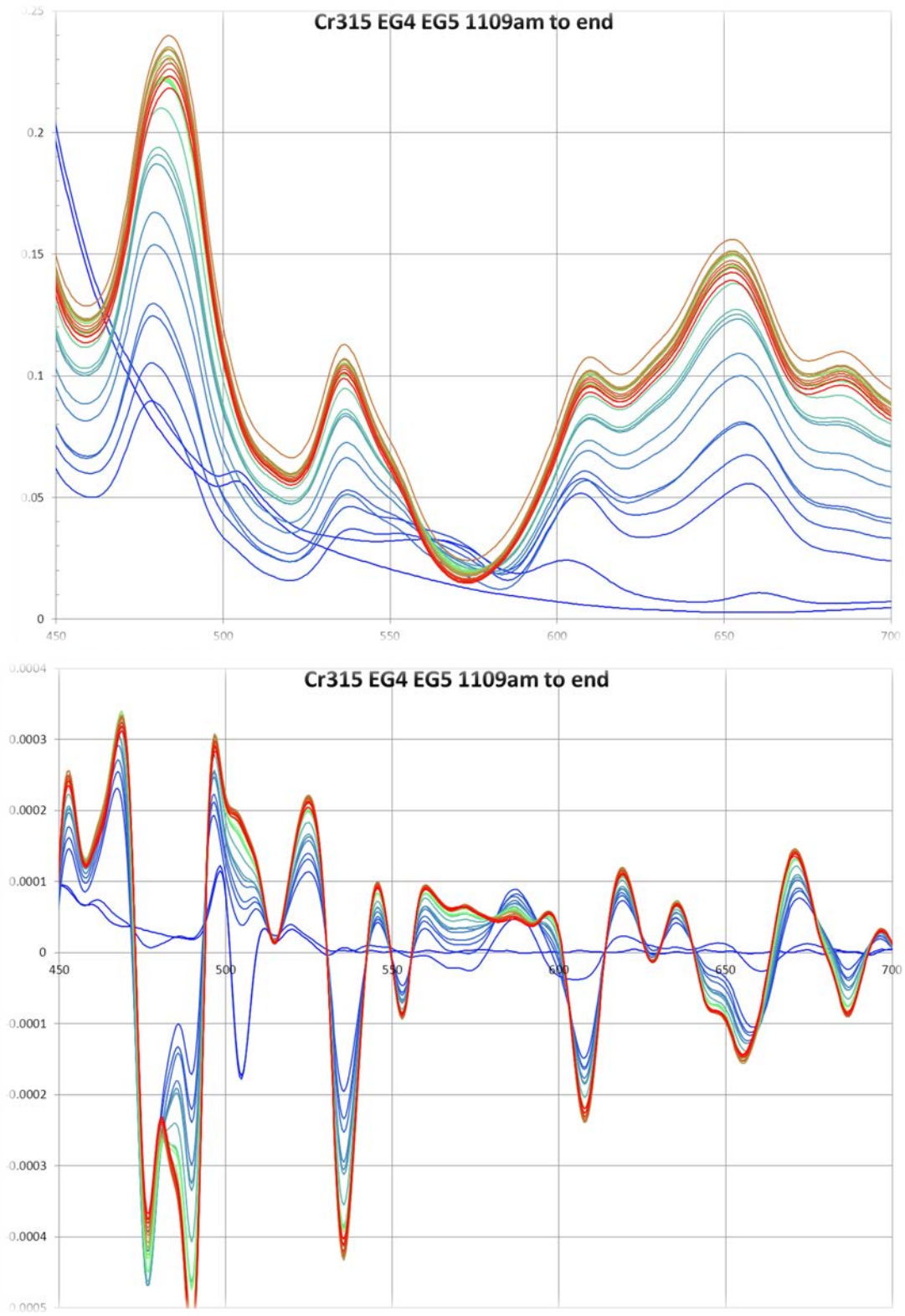

Figure 10d. Cr315 Spectra – 1105 mL (11.8 BV) , 1185 mL (13.9 BV) and 1367mL (15.6 BV) to End of Wash.

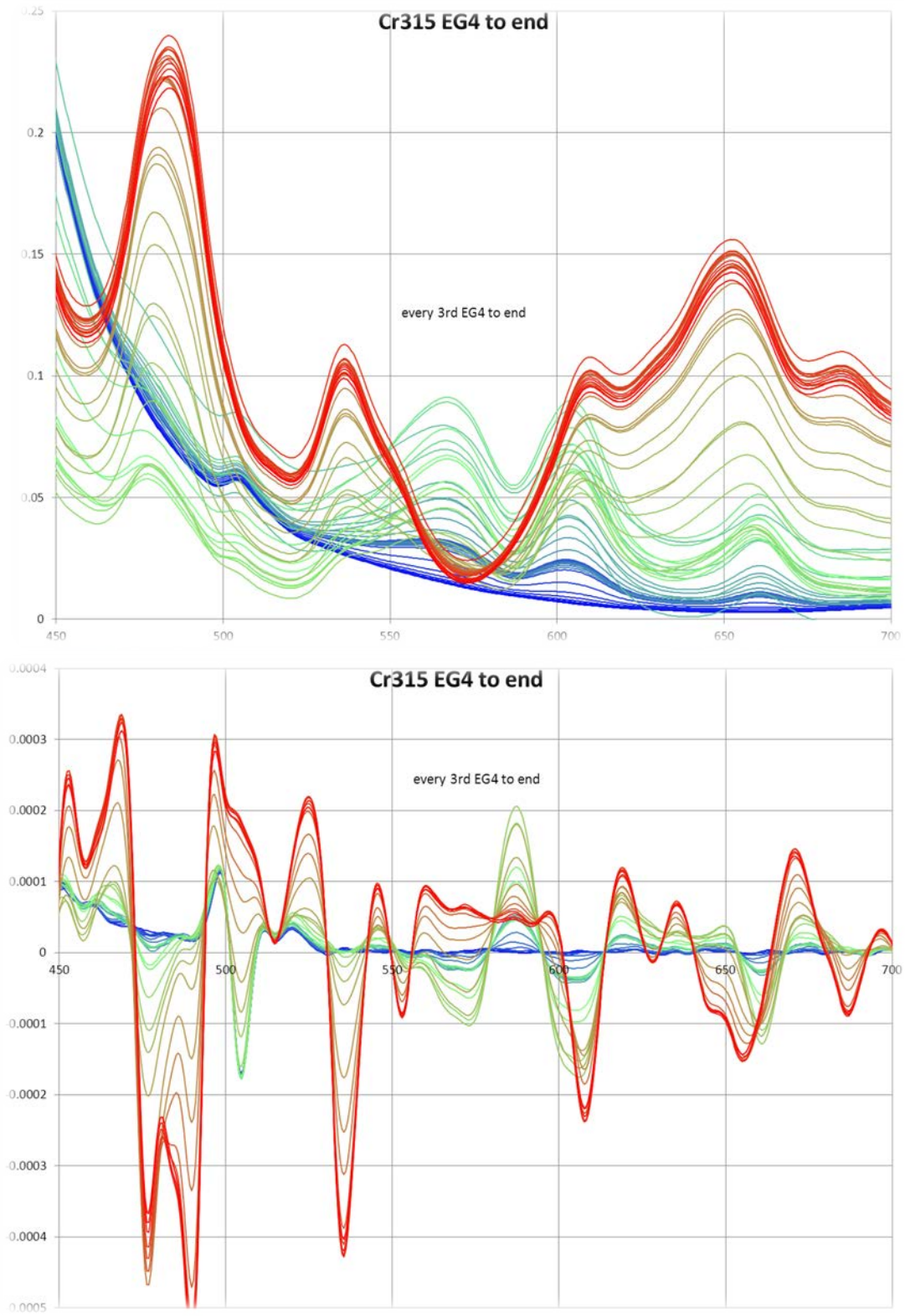

Figure 10e. Cr315 Spectra – 1105 mL (11.8 BV) to End of Wash (every 3rd Spectra).

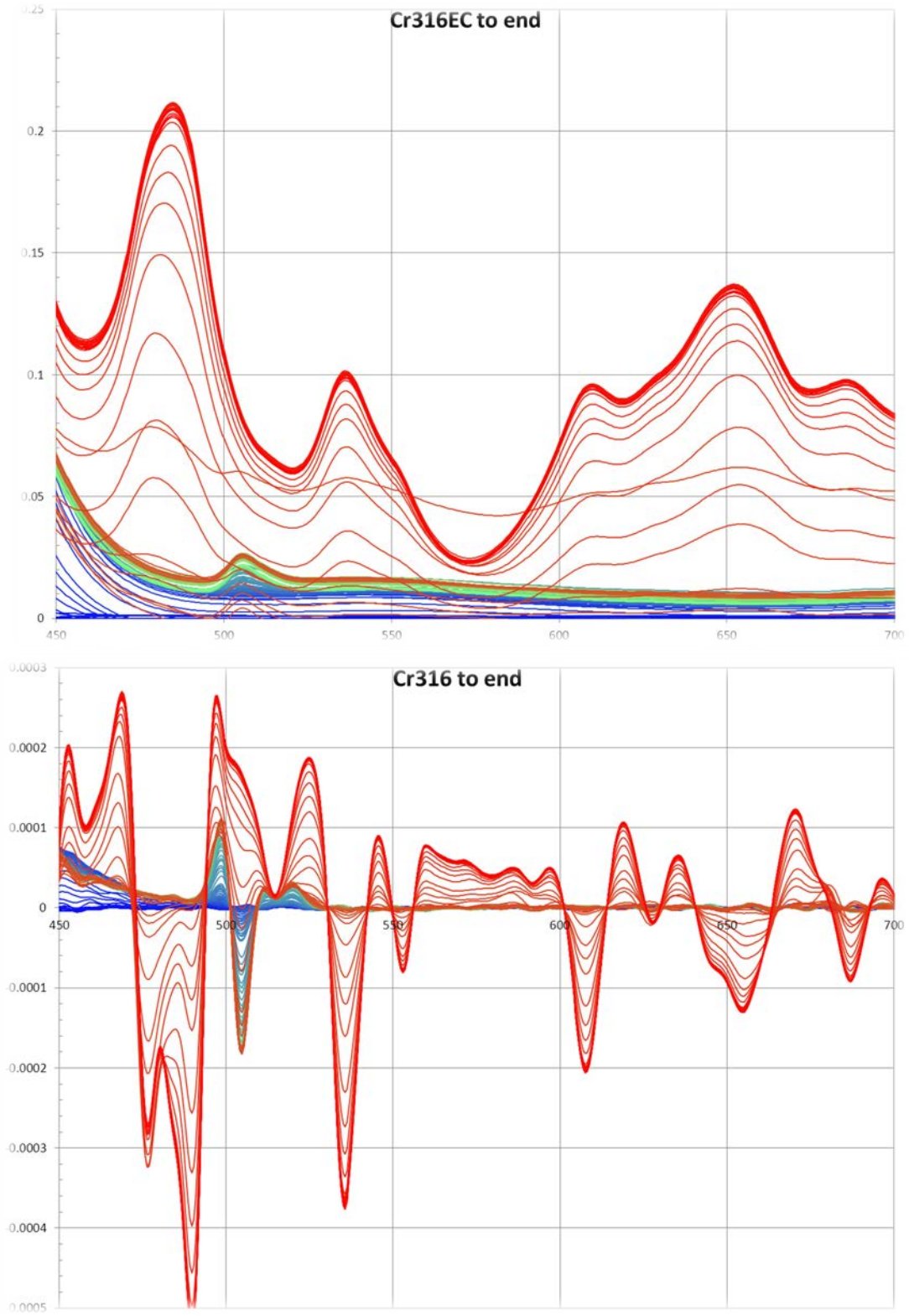

Figure 11a. Cr316 Spectra – Overview.

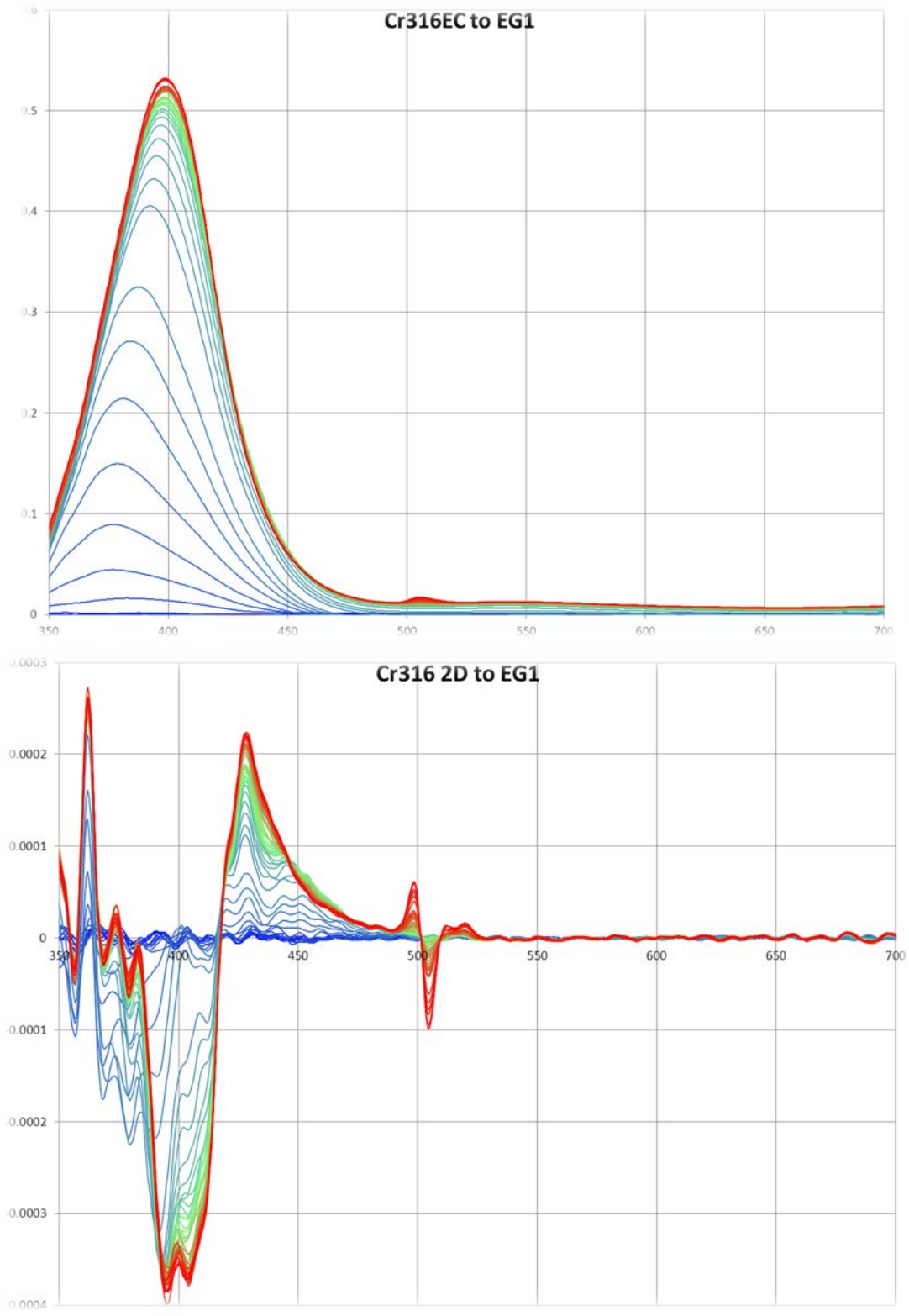

Figure 11b. Cr316 Spectra – Start to 250mL (2.9 BV).

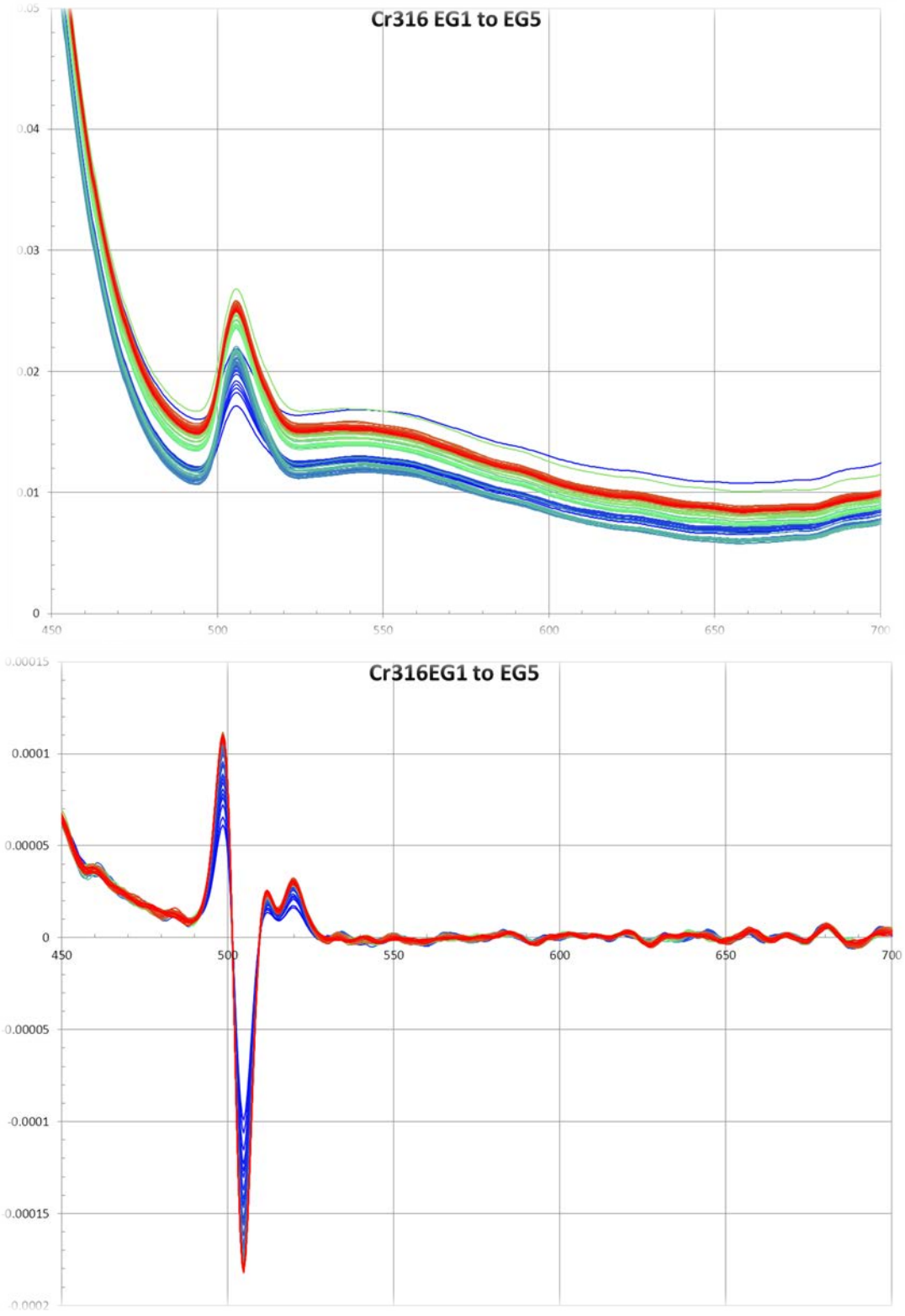

Figure 11c. Cr316 Spectra – 250mL (2.9 BV) to 1159mL (13.6 BV).

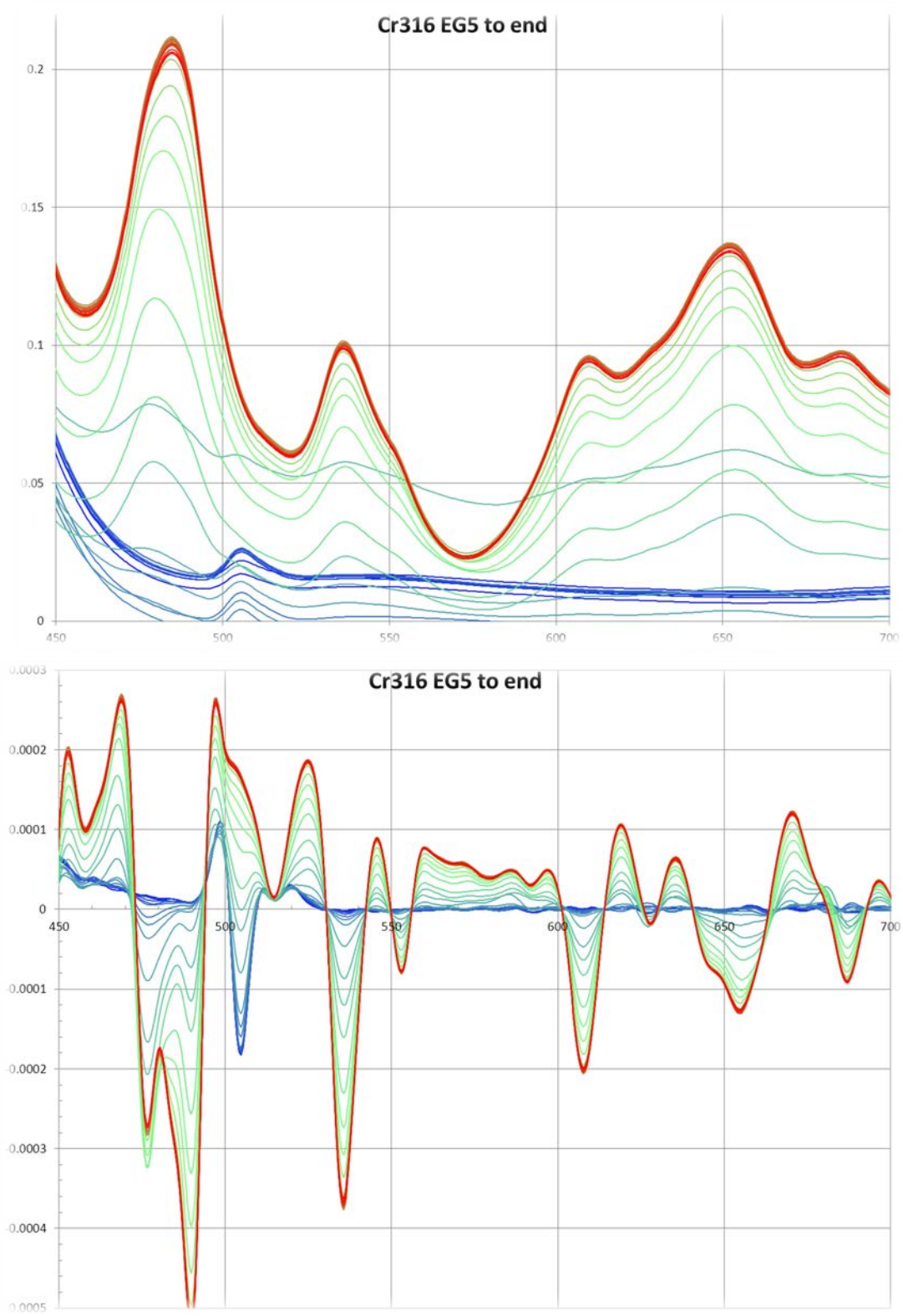

Figure 11d. Cr316 Spectra – 1159 mL (13.6 BV) to End of Wash.

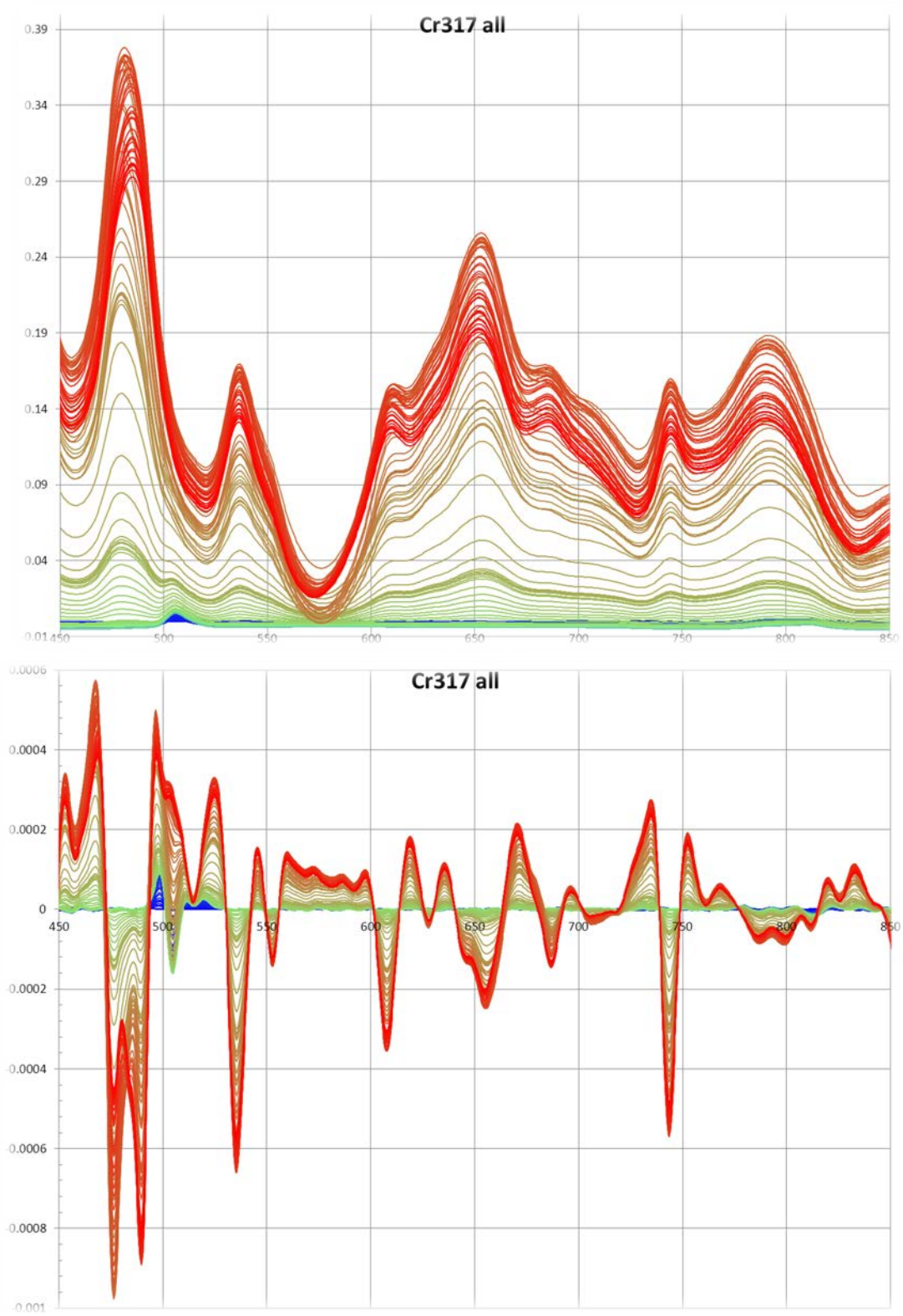

Figure 12a. Cr317 Spectra – Overview.

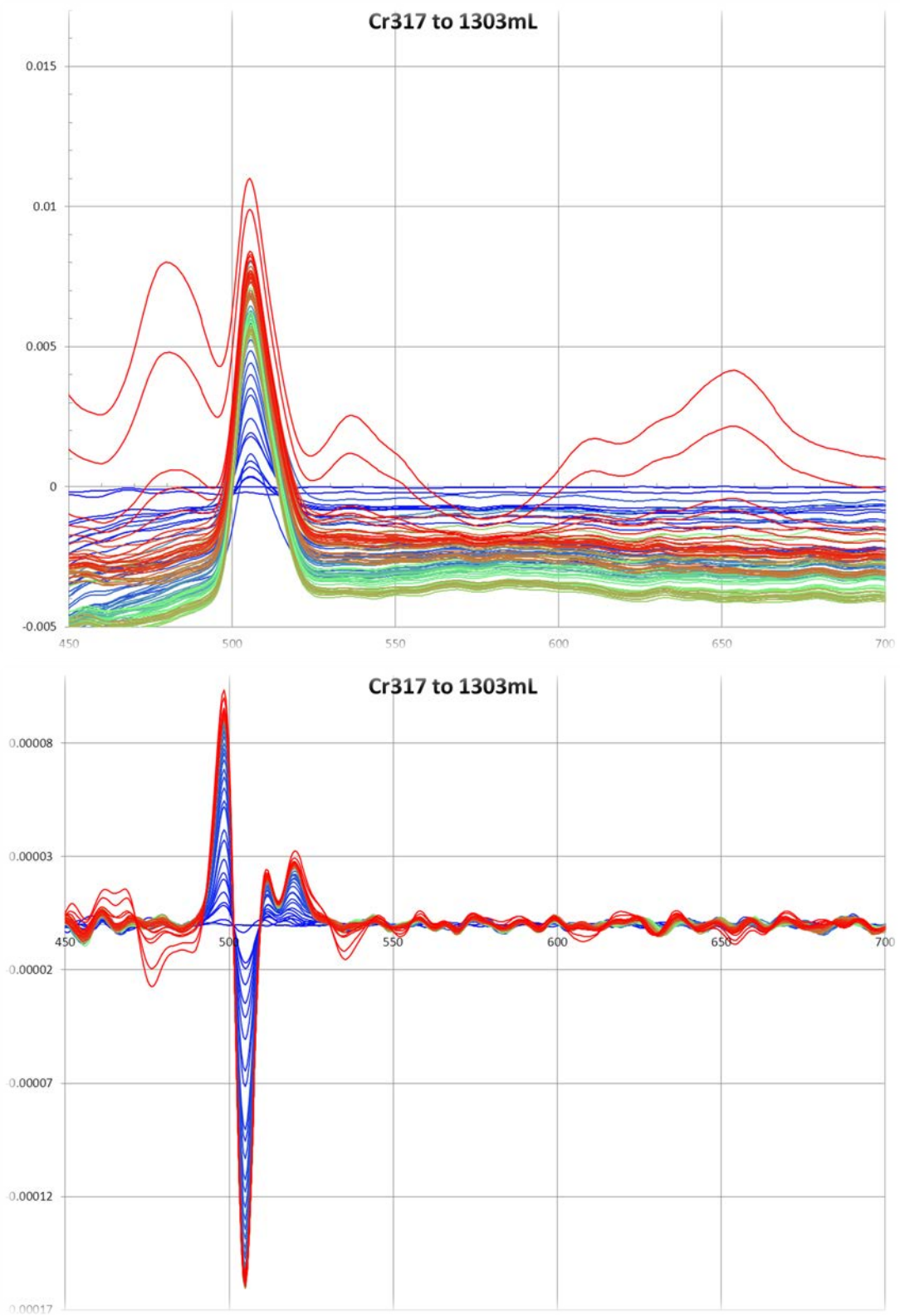

Figure 12b. Cr317 Spectra – Start to 1303 mL (15.2 BV).

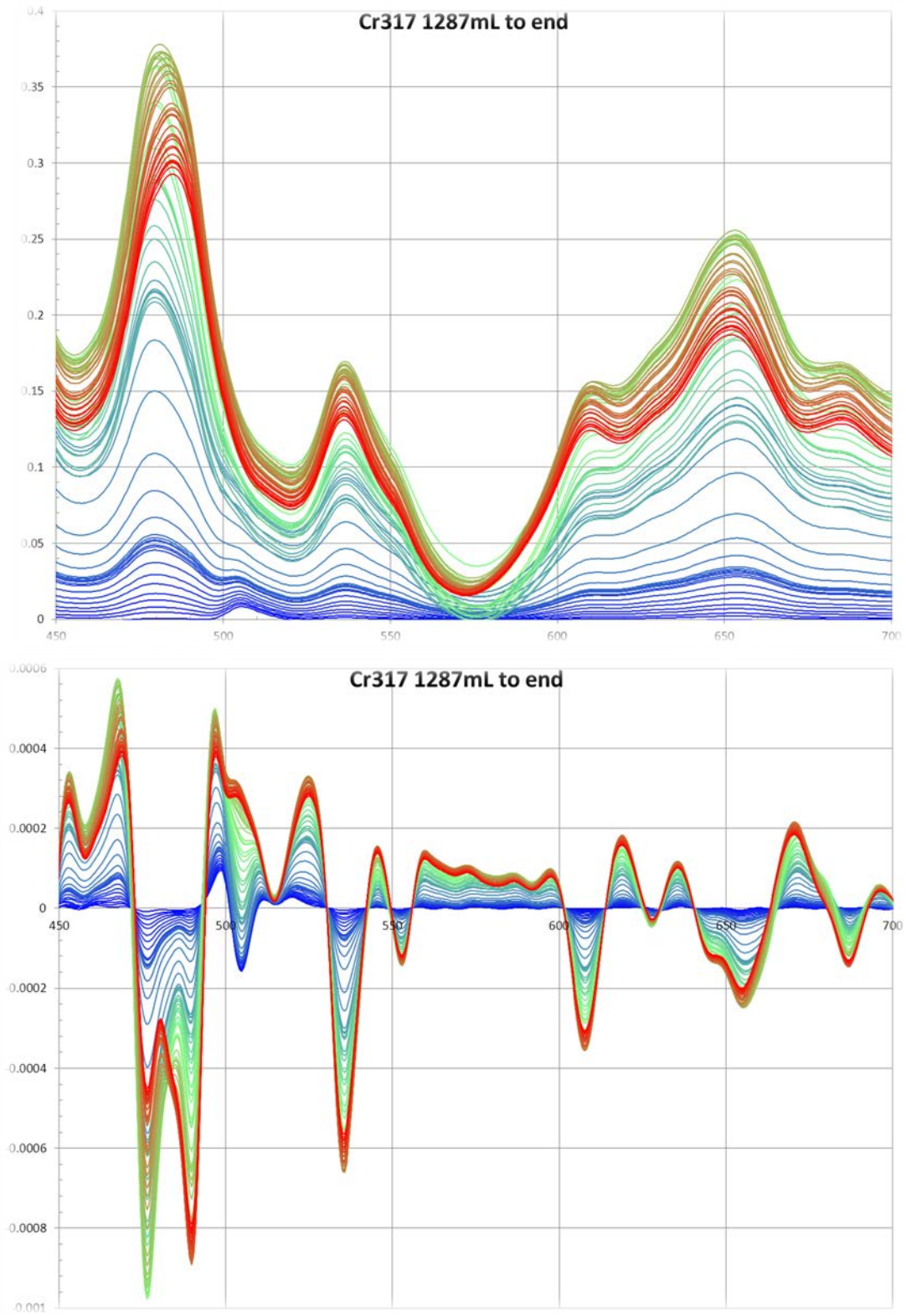

Figure 12c. Cr317 Spectra – 1287 mL (15.1 BV) to End of Wash.

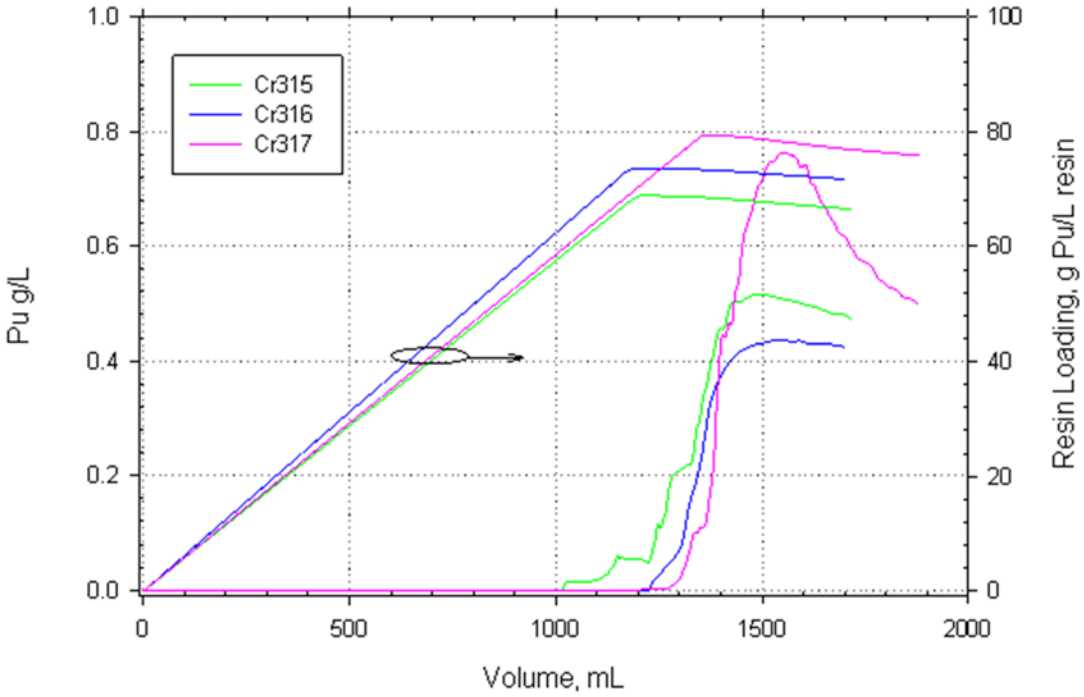

Figure 13. Plot of Resin Loading and Raffinate/Wash Pu Losses as a Function of Volume.

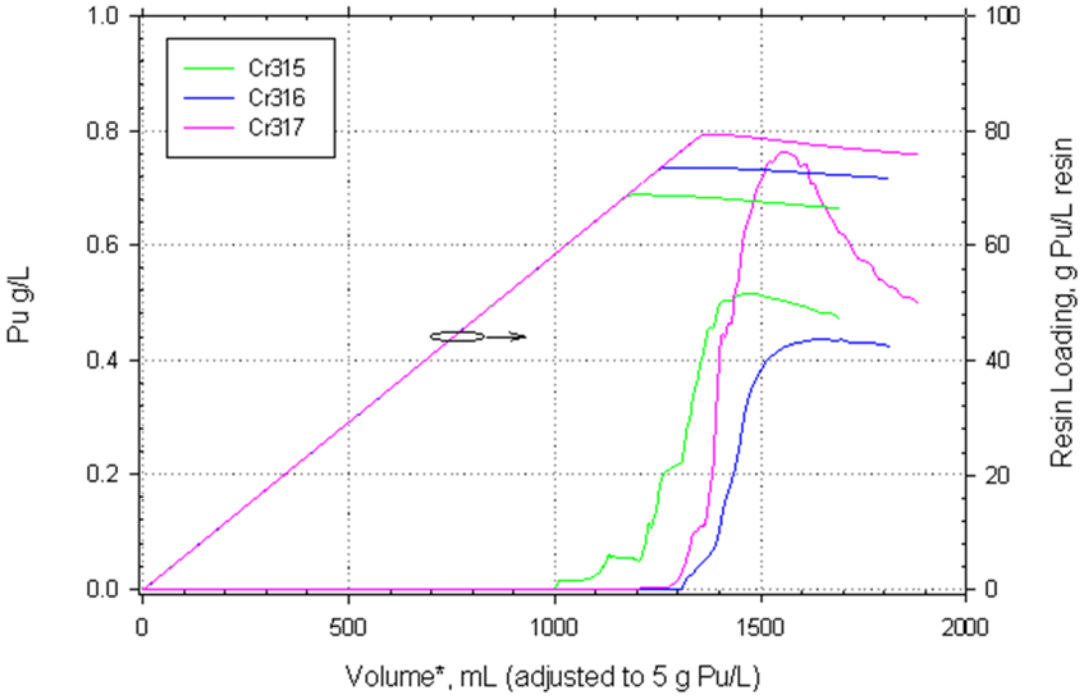

Figure 14. Plot of Resin Loading and Raffinate/Wash Pu Losses as a Function of Adjusted Volume.

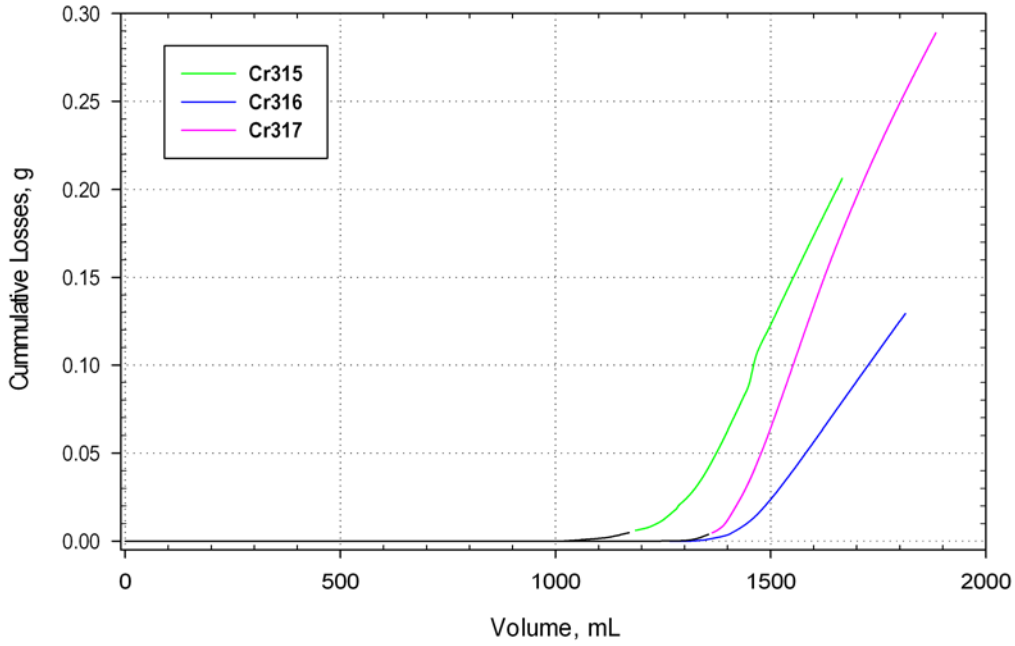

Figure 15. Plot of Cumulative Pu Losses as a Function of Volume.

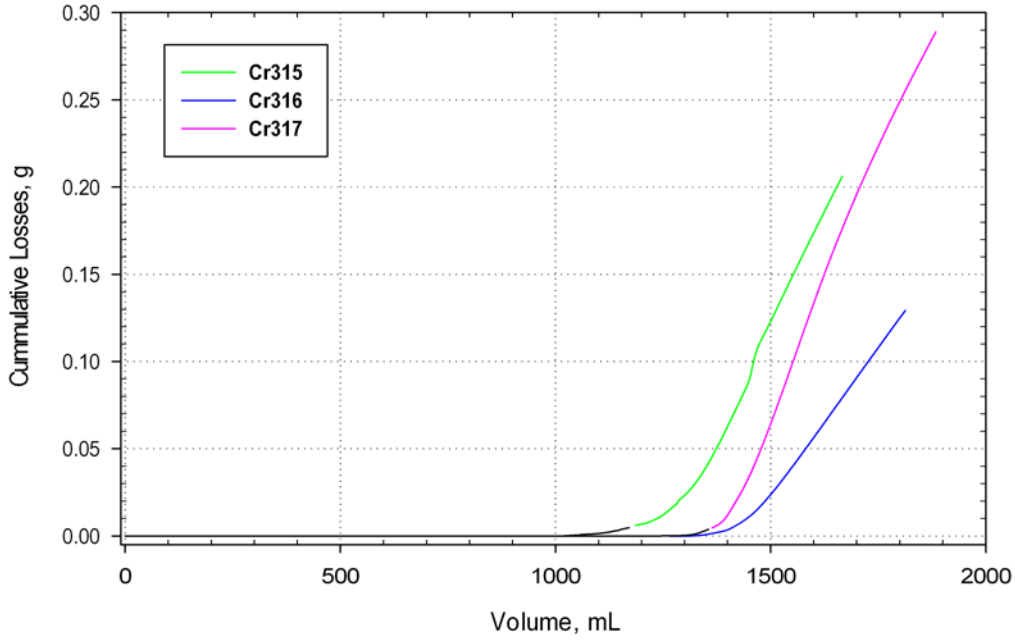

Figure 16. Plot of Cumulative Pu Losses as a Function of Adjusted Volume.

Distribution:

S. D. Fink, 773-A
K. M. Fox, 999-W
B. J. Giddings, 786-5A
C. C. Herman, 999-W
S. L. Marra, 773-A
F. M. Pennebaker, 773-42A
W. R. Wilmarth, 773-A
W. E. Harris, 704-2H
J. B. Schaade, 704-2H
G. J. Zachman, 225-7H
P. B. Andrews, 704-2H
S. J. Howell, 704-3H
M. J. Swain, 703-H
M. J. Lewczyk, 221-H
K. P. Burrows, 704-2H
J. E. Therrell, 704-2H
J. W. Christopher, 704-2H
J. E. Elkourie, 704-2H
A. T. Masterson, 704-2H
R. H. Smith, 704-2H
R. R. Livingston, 730-2B
J. L. O'Conner, 105-L
W. G. Dyer, 704-2H
S. L. Hudlow, 221-H
W. H. Clifton, 704-2H
S. L. Garrison, 704-2H
E. A. Kyser, 773-A
T. S. Rudisill, 773-A
R. A. Pierce, 773-A
M. L. Crowder, 773-A
P. E. O'Rourke, 773-A
W. D. King, 773-42A
M. C. Thompson, 773-A
B. J. Wiedenman, 773-A
T. L. White, 773-A
W. L. Melton, 707-F
S. A. Thomas, 703-46A